Module
1.7

Optical Waveguides and Fibers

Ajoy Ghatak and K. Thyagarajan
Department of Physics
Indian Institute of Technology
New Delhi, India

The dramatic reduction of transmission loss in optical fibers coupled with equally important developments in the area of light sources and detectors has brought about a phenomenal growth of the fiber optic industry during the past two decades. The birth of optical fiber communication coincided with the fabrication of low-loss optical fibers and room-temperature operation of semiconductor lasers in 1970. Ever since, the scientific and technological progress in this field has been so phenomenal that we are already in the fifth generation of optical fiber communication systems within a brief span of 30 years. Recent developments in optical amplifiers and wavelength division multiplexing (WDM) are taking us to a communication system with almost "zero" loss and "infinite" bandwidth. Indeed, optical fiber communication systems are fulfilling the increased demand on communication links, especially with the proliferation of the Internet. This module, *Optical Waveguides and Fibers,* is an introduction to the basics of fiber optics, discussing especially the characteristics of optical fibers as regards their application to telecommunication (to be covered in Module 1.8, *Fiber Optic Telecommunication*) and fiber optic sensors.

Prerequisites

Prior to the module, you are expected to have covered Modules 1-1, *Nature and Properties of Light*; Module 1-2, *Light Sources and Laser Safety*; Module 1-3, *Basic Geometrical Optics*; and Module 1-4, *Basic Physical Optics*. In addition, you should be able to manipulate and use algebraic formulas involving trigonometric functions and deal with units.

Objectives

The objective of the module is to present the basic characteristics of optical fibers that are important from the point of view of their applications in telecommunication and sensing. Characteristics such as attenuation, pulse dispersion, single-mode and multimode fibers, graded-index, fibers and zero-dispersion wavelength are covered.

When you finish this module, you will be able to

- Describe how light is guided through optical fibers.
- Differentiate between multimode and single-mode fibers.
- Calculate the numerical aperture (*NA*), intermodal dispersion, and material dispersion.
- Understand zero-dispersion wavelength and dispersion-shifted fibers.
- Know the importance of plastic optical fibers with regard to their application in communication.
- Describe how optical fibers can be used in sensing.

Fiber Optics as a Career

*Although not apparent, fiber optics plays a very significant role in our daily lives. When we make long-distance or international telephone calls or browse through the Internet, we are communicating through optical fibers. Without a backbone of an optical fiber network, it would be almost impossible to have all the current facilities of communication and information transfer. The entire world is being "*fibered*." Having a basic understanding of the guiding properties of optical fibers and recognizing their applications in communication and sensing can provide a person with an added advantage in terms of job prospects in many different areas. Fiber optics is being used in diverse applications such as cold lighting in museums, construction of smart civil structures, and networking for communication. Among many issues associated with day-to-day handling of optical fibers, a fiber optic technician may have to solve problems regarding joining of optical fibers, location of fiber breaks, and fiber end preparation. The field of fiber optics is as exciting as ever and continues to expand even faster than microelectronics. The true age of optics, in which fiber optics is a very important part, is here and is expected to contribute in making the 21st century the century of photonics.*

Abbreviations

CSF	Conventional single-mode fiber
DSF	Dispersion-shifted fiber
FOG	Fiber optic gyroscope
LD	Laser diode
LED	Light-emitting diode
MMF	Multimode fiber
NA	Numerical aperture
nm	Nanometer
Pa	Pascal
PIF	Parabolic-index fiber
POF	Plastic optical fiber
ps	Picosecond
SIF	Step-index fiber
TIR	Total internal reflection
WDM	Wavelength-division multiplexing

Opening Demonstrations

Fiber optics is an exciting field, and the demonstration exercises that follow are sure to kindle one's interest in this fascinating area.

1. **Demonstration of light guidance through optical fibers**. Take a 2-meter length or so of optical fiber—preferably a large-diameter plastic optical fiber—and make perpendicular cuts at both the ends. Couple light from a laser pointer into one of the ends and see for

yourself how the light is guided through the fiber. If the room is dark, you should be able to observe the entire fiber glowing all along its length due to scattering (Rayleigh scattering). Observe the light emerging from the other end of the fiber. Try tying the fibers in a knot and you will notice that light still is guided, in spite of the severe bend of the fiber. If you use a long reel of the optical fiber, you should still see the emerging light at the other end and the glow along the entire reel. Figure 7-1 shows a photograph of light propagating through a long optical fiber.

Figure 7-1 *A long, thin optical fiber transmitting a light beam (Photograph courtesy Dr. Chynoweth)*

2. **Differentiate between two kinds of fibers**. Take short pieces (~ 2 m) of a multimode optical fiber and a single-mode optical fiber. Focus the light from a HeNe laser onto the input end of the fiber using a lens such as a microscope objective, and observe the output by projecting it onto a white screen. The output from the multimode fiber will show a speckle pattern while that from a single-mode fiber will show a very uniform beam much like the output from a good laser. In the former case, the light propagates via a large number of modes, and the interference between the various modes causes the speckle pattern.
3. **Simple demonstration of sensing property of optical fibers**. Perform the previous demonstration using a multimode fiber reel by fixing the entire setup on a table and observing the output speckle pattern as you bring your hand close to the optical fiber reel. The warmth of the hand is enough to change the phase difference between the interfering modes, which in turn changes the interference pattern. The speckle pattern will keep changing as you move your hand closer to and farther from the reel. If you try to press or twist the fiber, you will immediately notice the change in the speckle pattern. Such changes in the pattern due to external influence demonstrate in a very simple fashion the possibility of using optical fibers for sensing.
4. **Demonstration of Rayleigh scattering in an optical fiber.** Rayleigh scattering is responsible for the blue color of the sky and the red color of the setting sun. It is very interesting to demonstrate the wavelength dependence of Rayleigh scattering using a long optical fiber. Couple white light from a lamp, such as a tungsten halogen lamp emitting white light, into a 1-km length or so of multimode optical fiber and look into the output.

Notice the color of the light. Cut the fiber, leaving about 1 m from the input end of the fiber, and repeat the experiment with this 1 m of fiber. You will see that, in the former case, the emerging light looks reddish while in the latter case it looks white. This difference is due to the *decrease of loss* with *increase in wavelength* due to Rayleigh scattering. Thus, shorter wavelengths toward the blue region have suffered greater scattering out of the fiber than longer wavelengths near the red region. Even though all wavelengths at the input end are coupled, there is more power in the red part at the output end, thereby giving the light a reddish color.

Basic Concepts

I. HISTORICAL INTRODUCTION

Communication implies transfer of information from one point to another. When it is necessary to transmit information, such as speech, images, or data, over a distance, one generally uses the concept of carrier wave communication. In such a system, the information to be sent modulates an electromagnetic wave such as a radio wave, microwave, or light wave, which acts as a carrier. This modulated wave is then transmitted to the receiver through a channel and the receiver demodulates it to retrieve the imprinted signal. The carrier frequencies associated with TV broadcast (~ 50–900 MHz) are much higher than those associated with AM radio broadcast (~ 600 kHz–20 MHz). This is due to the fact that, in any communication system employing electromagnetic waves as the carrier, **the amount of information that can be sent increases as the frequency of the carrier is increased.**[1] Obviously, TV broadcast has to carry much more information than AM broadcasts. Since optical beams have frequencies in the range of 10^{14} to 10^{15} Hz, the use of such beams as the carrier would imply a tremendously large increase in the information-transmission capacity of the system as compared to systems employing radio waves or microwaves.

In a conventional telephone hookup, voice signals are converted into equivalent electrical signals by the microphone and are transmitted as electrical currents through metallic (copper or aluminum) wires to the local telephone exchange. Thereafter, these signals continue to travel as electric currents through metallic wire cable (or for long-distance transmission as radio/microwaves to another telephone exchange) usually with several repeaters in between. From the local area telephone exchange, at the receiving end, these signals travel via metallic wire pairs to the receiver telephone, where they are converted back into corresponding sound waves. Through such cabled wire-pair telecommunication systems, one can at most send 48 simultaneous telephone conversations intelligibly. On the other hand, in an optical communication system that uses glass fibers as the transmission medium and light waves as carrier waves, it is distinctly possible today to have 35,000 or more simultaneous telephone

[1] The information-carrying capacity of an electromagnetic carrier is approximately proportional to the difference between the maximum and the minimum frequencies (technically known as *bandwidth* of the channel) that can be transmitted through the communication channel. The higher one goes in the electromagnetic spectrum in frequency scale, the higher the bandwidth and hence the information-carrying capacity of such a communication system. That is why historically the trend in carrier wave communication has been always toward bandwidths of higher and higher frequencies.

conversations (equivalent to a transmission speed of about 2.5 Gbit/s) through one glass fiber no thicker than a human hair. This large information-carrying capacity of a light beam is what generated interest among communication engineers and caused them to explore the possibility of developing a communication system using light waves as carrier waves.

The idea of using light waves for communication can be traced as far back as 1880 when Alexander Graham Bell invented the photophone (see Figure 7-2) shortly after he invented the telephone in 1876. In this remarkable experiment, speech was transmitted by modulating a light beam, which traveled through air to the receiver. The flexible reflecting diaphragm (which could be activated by sound) was illuminated by sunlight. The reflected light was received by a parabolic reflector placed at a distance of about 200 m. The parabolic reflector concentrated the light on a photoconducting selenium cell, which formed a part of a circuit with a battery and a receiving earphone. Sound waves present in the vicinity of the diaphragm vibrated the diaphragm, which led to a consequent variation of the light reflected by the diaphragm. The variation of the light falling on the selenium cell changed the electrical conductivity of the cell, which in turn changed the current in the electrical circuit. This changing current reproduced the sound on the earphone.

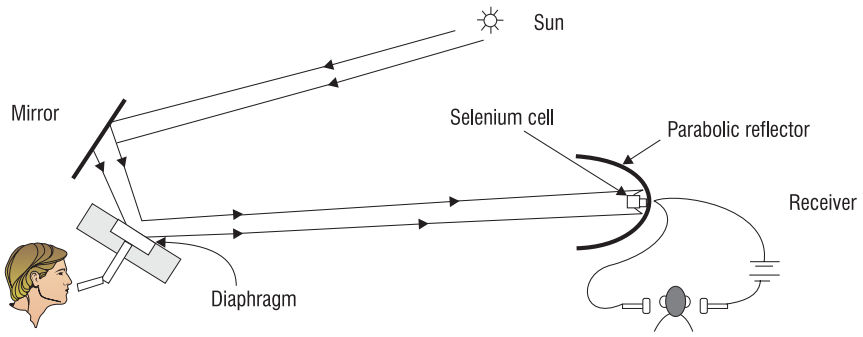

Figure 7-2 *Schematic of the photophone invented by Bell. In this system, sunlight was modulated by a vibrating diaphragm and transmitted through a distance of about 200 meters in air to a receiver containing a selenium cell connected to the earphone.*

After succeeding in transmitting a voice signal over 200 meters using a light signal, Bell wrote to his father: "I have heard a ray of light laugh and sing. We may talk by light to any visible distance without any conducting wire." To quote from Maclean: "In 1880 he (Graham Bell) produced his 'photophone' which to the end of his life, he insisted was '…. the greatest invention I have ever made, greater than the telephone…' Unlike the telephone, though, it had no commercial value."

The modern impetus for telecommunication with carrier waves at optical frequencies owes its origin to the discovery of the laser in 1960. Earlier, no suitable light source was available that could reliably be used as the information carrier.[2] At around the same time, telecommunication traffic was growing very rapidly. It was conceivable then that conventional telecommunication systems based on, say, coaxial cables, radio and microwave links, and wire-pair cable, could soon reach a saturation point. The advent of lasers immediately triggered a great deal of

[2] We may mention here that, although incoherent sources like light-emitting diodes (LED) are also often used in present-day optical communication systems, it was discovery of the laser that triggered serious interest in the development of optical communication systems.

investigation aimed at examining the possibility of building optical analogues of conventional communication systems. The very first such modern optical communication experiments involved laser beam transmission through the atmosphere. However, it was soon realized that shorter-wavelength laser beams could not be sent in open atmosphere through reasonably long distances to carry signals, unlike, for example, the longer-wavelength microwave or radio systems. This is due to the fact that a laser light beam (of wavelength about 1 μm) is severely attenuated and distorted owing to scattering and absorption by the atmosphere. Thus, for reliable light-wave communication under terrestrial environments it would be necessary to provide a "guiding" medium that could protect the signal-carrying light beam from the vagaries of the terrestrial atmosphere. This guiding medium is the optical fiber, a hair-thin structure that guides the light beam from one place to another as was shown in Figure 7-1. The guidance of the light beam through the optical fiber takes place because of total internal reflection, which we discuss in the following section.

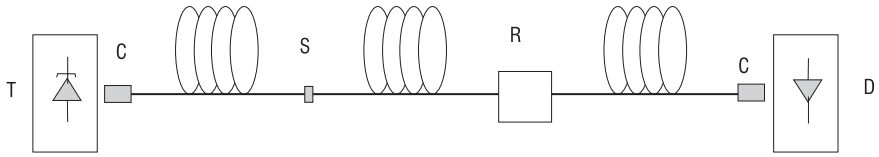

Figure 7-3 *A typical fiber optic communication system: T, transmitter; C, connector; S, splice; R, repeater; D, detector*

In addition to the capability of carrying a huge amount of information, optical fibers fabricated with recently developed technology are characterized by extremely low losses[3] (< 0.2 dB/km), as a consequence of which the distance between two consecutive repeaters (used for amplifying and reshaping the attenuated signals) could be as large as 250 km. We should perhaps mention here that it was the epoch-making paper of Kao and Hockham in 1966 that suggested that optical fibers based on silica glass could provide the necessary transmission medium if metallic and other impurities could be removed. Indeed, this 1966 paper triggered the beginning of serious research in developing low-loss optical fibers. In 1970, Kapron, Keck, and Maurer (at Corning Glass in USA) were successful in producing silica fibers with a loss of about 17 dB/km at a wavelength of 633 nm. (Kapron, Keck, and Maurer) Since then, the technology has advanced with tremendous rapidity. By 1985 glass fibers were routinely produced with extremely low losses (< 0.2 dB/km). Figure 7-3 shows a typical optical fiber communication system. It consists of a transmitter, which could be either a laser diode or an LED, the light from which is coupled into an optical fiber. Along the path of the optical fiber are splices, which are permanent joints between sections of fibers, and repeaters that boost the signal and correct any distortion that may have occurred along the path of the fiber. At the end of the link, the light is detected by a photodetector and electronically processed to retrieve the signal.

II. TOTAL INTERNAL REFLECTION (TIR)

At the heart of an optical communication system is the optical fiber that acts as the transmission channel carrying the light beam loaded with information. As mentioned earlier, the guidance of

[3] Attenuation is usually measured in decibels (dB).We define attenuation in Section VI.

the light beam (through the optical fiber) takes place because of the phenomenon of total internal reflection (TIR), which we will now discuss. You learned about critical angles, TIR, etc. in Module 1-3, *Basic Geometrical Optics*. You need now to refresh your memory and apply these ideas more directly to the physics of optical fibers. We first define the refractive index (n) of a medium:

$$n = \frac{c}{v} \tag{7-1}$$

where c ($\approx 3 \times 10^8$ m/s) is the speed of light in free space and v represents the velocity of light in that medium. For example, for light waves, $n \approx 1.5$ for glass and $n \approx 1.33$ for water.

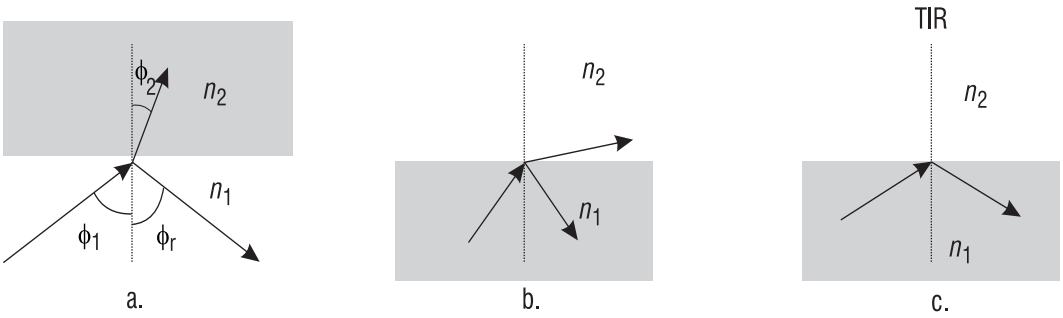

Figure 7-4 (a) *A ray of light incident on a denser medium* ($n_2 > n_1$). (b) *A ray incident on a rarer medium* ($n_2 < n_1$). (c) *For* $n_2 < n_1$ *, if the angle of incidence is greater than critical angle, it will undergo total internal reflection.*

As you know, when a ray of light is incident at the interface of two media (like air and glass), the ray undergoes partial reflection and partial refraction as shown in Figure 7-4a. The vertical dotted line represents the normal to the surface. The angles ϕ_1, ϕ_2, and ϕ_r represent the angles that the incident ray, refracted ray, and reflected ray make with the normal. According to Snell's law and the law of reflection,

$$n_1 \sin \phi_1 = n_2 \sin \phi_2 \quad \text{and} \quad \phi_1 = \phi_2 \tag{7-2}$$

Further, the incident ray, reflected ray, and refracted ray lie in the same plane. In Figure 7-4a, since $n_2 > n_1$ we must have (from Snell's law) $\phi_2 < \phi_1$, i.e., the ray will bend toward the normal. On the other hand, if a ray is incident at the interface of a rarer medium ($n_2 < n_1$), the ray will bend away from the normal (see Figure 7-4b). The angle of incidence, for which the angle of refraction is 90°, is known as the critical angle and is denoted by ϕ_c . Thus, when

$$\phi_1 = \phi_c = \sin^{-1}\left(\frac{n_2}{n_1}\right) \tag{7-3}$$

$\phi_2 = 90°$. When the angle of incidence exceeds the critical angle (i.e., when $\phi_1 > \phi_c$), there is no refracted ray and we have total internal reflection (see Figure 7-4c).

Example 7-1

For the glass-air interface, $n_1 = 1.5$, $n_2 = 1.0$, and the critical angle is given by

$$\phi_c = \sin^{-1}\left(\frac{1}{1.5}\right) \approx 41.8°$$

On the other hand, for the glass-water interface, $n_1 = 1.5$, $n_2 = 1.33$, and

$$\phi_c = \sin^{-1}\left(\frac{1.33}{1.5}\right) \approx 62.5°.$$

The phenomenon of total internal reflection can be very easily demonstrated through a simple experiment as shown in Figure 7-5. A thick, semicircular glass disc is immersed in a glass vessel filled with water. A laser beam from a HeNe laser or a laser pointer is directed toward the center of the semicircular disc so that it is incident normally on the glass surface and goes undeviated toward *O* as shown in the figure. The angle of incidence (at the water-glass interface) is increased by rotating the glass disc about the point *O,* always keeping the incident ray normal to the circular disc. Eventually, when the angle of incidence exceeds the critical angle (≈ 62.5°), the laser beam undergoes TIR —as shown in Figure 7-5. The ray trace can be clearly seen when viewed from the top. If one puts a drop of ink in the water, the light path becomes very beautiful to look at! The experiment is very simple and we urge the reader to carry it out using a laser pointer.

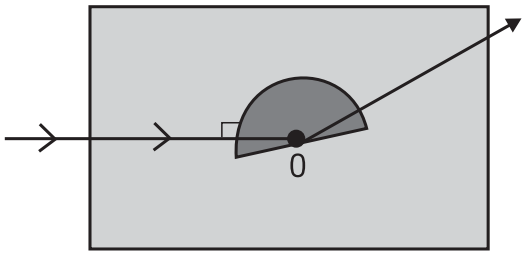

Figure 7-5 *A simple laboratory experiment to demonstrate the phenomenon of TIR*

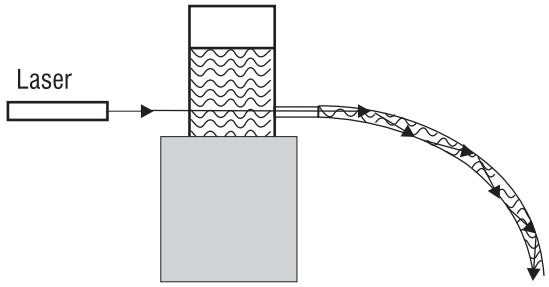

Figure7-6 *The concept of Tyndall's original experiment demonstrating the phenomenon of light guidance by TIR*

We should mention that the phenomenon of guidance by multiple total internal reflections was first demonstrated by John Tyndall in 1854. In this demonstration, Tyndall showed that light travels along the curved path of water emanating from an illuminated vessel (see Figure 7-6). Actually, light undergoes TIR at the water-air interface, along the water path, as shown in Figure 7-6.

III. THE OPTICAL FIBER

Figure 7-7a shows an optical fiber, which consists of a (cylindrical) central dielectric core clad by a material of slightly lower refractive index. The corresponding refractive index distribution (in the transverse direction) is given by:

$$\begin{aligned} n &= n_1 \quad \text{for} \quad r < a \\ n &= n_2 \quad \text{for} \quad r > a \end{aligned} \tag{7-4}$$

where n_1 and $n_2\,(<n_1)$ represent respectively the refractive indices of core and cladding and a represents the radius of the core. We define a parameter Δ through the following equations.

$$\Delta \equiv \frac{n_1^2 - n_2^2}{2n_2^2} \tag{7-5}$$

When $\Delta << 1$ (as is indeed true for silica fibers where n_1 is very nearly equal to n_2) we may write

$$\Delta = \frac{(n_1 + n_2)(n_1 - n_2)}{2n_1^2} \approx \frac{(n_1 - n_2)}{n_1} \approx \frac{(n_1 - n_2)}{n_2} \tag{7-6}$$

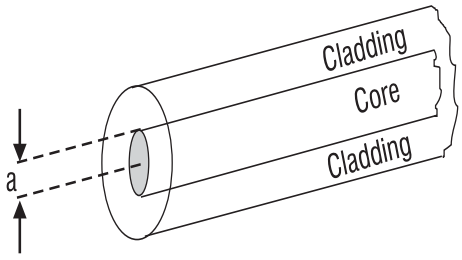

(a)

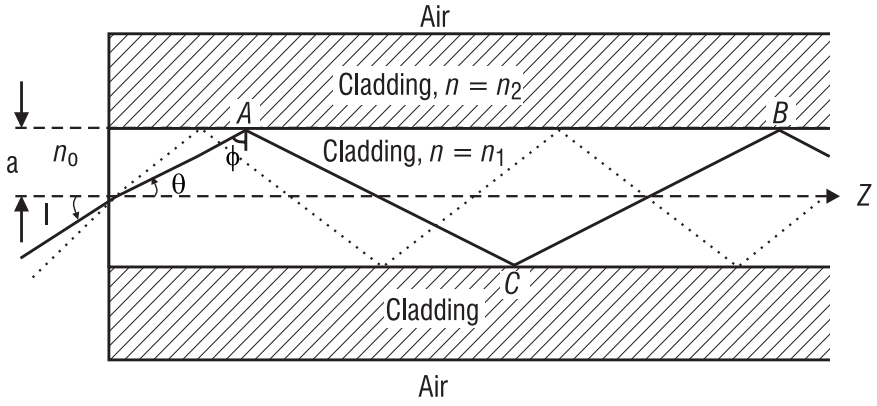

(b)

Figure 7-7 *(a) A glass fiber consists of a cylindrical central core clad by a material of slightly lower refractive index. (b) Light rays impinging on the core-cladding interface at an angle greater than the critical angle are trapped inside the core of the fiber.*

For a typical (multimode) fiber, $a \approx 25$ μm, $n_2 \approx 1.45$ (pure silica), and $\Delta \approx 0.01$, giving a core index of $n_1 \approx 1.465$. The cladding is usually pure silica while the core is usually silica doped with germanium. Doping by germanium results in a typical increase of refractive index from n_2 to n_1.

Now, for a ray entering the fiber core at its end, if the angle of incidence ϕ at the internal core-cladding interface is greater than the critical angle ϕ_c [$= \sin^{-1}(n_2/n_1)$], the ray will undergo TIR at that interface. Further, because of the cylindrical symmetry in the fiber structure, this ray will suffer TIR at the lower interface also and therefore be guided through the core by repeated total internal reflections. Even for a bent fiber, light guidance can occur through multiple total internal reflections (see Figures 7-1 and 7-6).

The necessity of a clad fiber (Figure 7-7)—rather than a bare fiber with no cladding—is clear. For transmission of light from one place to another, the fiber must be supported. Supporting structures, however, may considerably distort the fiber, thereby affecting the guidance of the light wave. This is avoided by choosing a sufficiently thick cladding. Further, in a fiber bundle, in the absence of the cladding, light can leak through from one fiber to another. The idea of adding a second layer of glass (namely, the cladding) came (in 1955) from Hopkins and Kapany in the United Kingdom. However, during that time the use of optical fibers was mainly in image transmission rather than in communication. Indeed, the early pioneering works in fiber optics (in the 1950s) were by Hopkins and Kapany in the United Kingdom and by Van Heel in Holland. Their work led to the use of the fibers in optical devices and medical instruments.

We may mention here that the retina of the human eye (see Module 1-2, *Light Sources and Safety,* and Module 1-6, *Optical Detectors and Human Vision*) consists of a large number of rods and cones that have the same kind of structure as the optical fiber. They consist of dielectric cylindrical rods surrounded by another dielectric of slightly lower refractive index. The core diameters are in the range of a few microns. The light absorbed in these "light guides" generates electrical signals, which are then transmitted to the brain through various nerves.

It is interesting to know why optical fibers are made of glass. Quoting from Professor W.A. Gambling, a pioneer in the field of fiber optics:

> We note that glass is a remarkable material which has been in use in 'pure' form for at least 9000 years. The compositions remained relatively unchanged for millennia and its uses have been widespread. The three most important properties of glass which makes it of unprecedented value are:
>
> 1. First, there is a wide range of accessible temperatures where its viscosity is variable. The viscosity can be controlled—unlike most materials, like water and metals, which remain liquid until they are cooled down to their freezing temperatures and then suddenly become solid. Glass, on the other hand, does not solidify at a discrete freezing temperature but gradually becomes stiffer and stiffer and eventually becomes hard. In the transition region it can be easily drawn into a thin fiber.
> 2. The second most important property is that highly pure silica is characterized with extremely low light transmission loss; i.e., it is highly transparent. Today, in most commercially available silica fibers, 96% of the power gets transmitted after propagating through 1 km of optical fiber. This indeed represents a truly remarkable achievement.

3. The third most remarkable property is the intrinsic strength of glass. It can support a stress of about 2,000,000 lb/in^2 so that a glass fiber of the type used in the telephone network with a diameter (125 μm) of twice the thickness of a human hair, can support a load of 40 pounds.

IV. THE COHERENT BUNDLE

A large number of fibers put together form what is known as a bundle. If the fibers are not aligned, i.e. they are all jumbled up, the bundle is said to be an *incoherent bundle*. However, if the fibers are aligned properly, i.e., if the relative positions of the fibers in the input and output ends are the same, the bundle is said to be a *coherent bundle*. If a particular fiber in this coherent bundle is illuminated at one of its ends, there will be a bright spot at the other end of the **same** fiber. Thus a coherent bundle will transmit the image from one end to another (see Figure 7-8). On the other hand, in an incoherent bundle the output image will be scrambled. Because of this property, an incoherent bundle can be used as a coder; the transmitted image can be decoded by using a similar bundle at the output end. In a bundle, since there can be hundreds of thousands of fibers, decoding without the original bundle configuration would be extremely difficult. Incoherent bundles are also used in illumination such as in traffic lights or road signs [see, e.g., "Schott Is Lighting the Way Home"] or even for lighting applications in buildings wherein the light source is removed from relatively inaccessible areas and fibers are used to guide light from a lamp [see, e.g., "Fiber Optic Technology Put to Work—Big Time"]. They can also be used as cold light sources (i.e., light sources giving only light and no heat) by cutting off the heat radiation with a filter at the input to the fiber bundle. The light emerging from the bundle is also free from UV radiation and is suitable for illumination of paintings in museums.

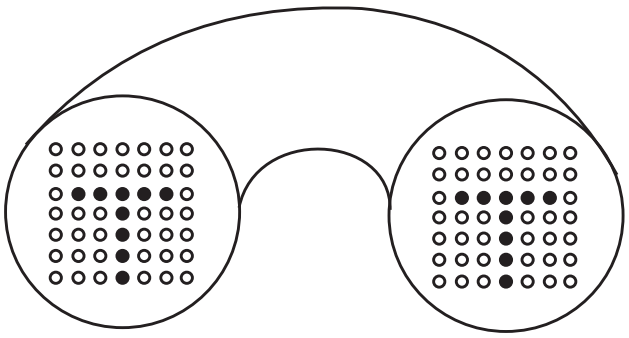

Figure 7-8 *A bundle of aligned fibers. A bright (or dark) spot at the input end of the coherent fiber bundle produces a bright (or dark) spot at the output end. Thus, an image will be transmitted (in the form of bright and dark spots) through a bundle of aligned fibers, forming, for example, the letter* T *shown above.*

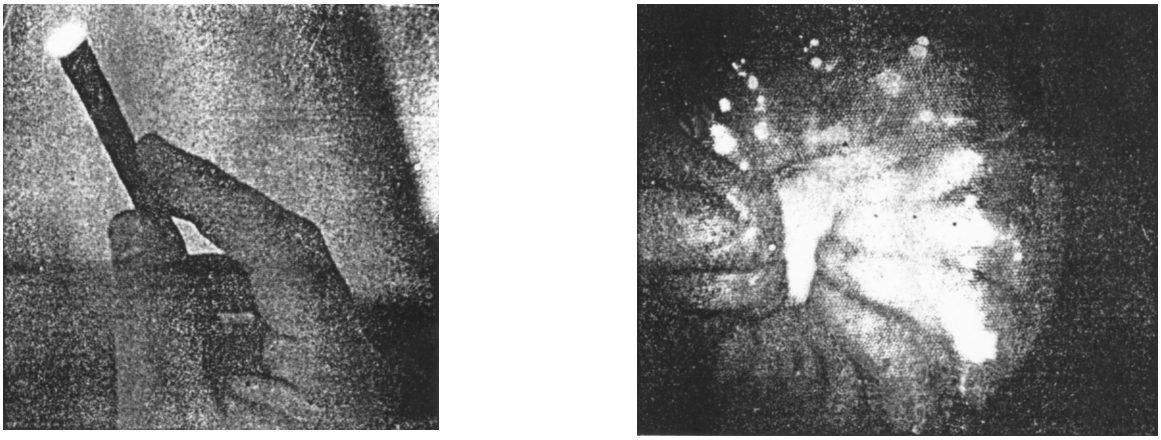

Figure 7-9 *(a) An optical fiber medical probe called an endoscope enables doctors to examine the inner parts of the human body. (b) A stomach ulcer as seen through an endoscope [Photographs courtesy United States Information Service, New Delhi]*

Perhaps the most important application of a coherent bundle is in a fiber optic endoscope where it can be inserted inside a human body and the interior of the body can be viewed from outside. For illuminating the portion that is to be seen, the bundle is enclosed in a sheath of fibers that carry light from outside to the interior of the body (see Figure 7-9). A state-of-the-art fiberscope can have about 10,000 fibers, which would form a coherent bundle of about 1 mm in diameter, capable of resolving objects 70 μm across. Fiber optic bundles can also be used for viewing internal machine parts that are otherwise inaccessible.

V. THE NUMERICAL APERTURE (NA)

We return to Figure 7-7b and consider a ray that is incident on the entrance face of the fiber core, making an angle i with the fiber axis. Let the refracted ray make an angle θ with the same axis. Assuming the outside medium to have a refractive index n_0 (which for most practical cases is unity), we get

$$\boxed{\frac{\sin i}{\sin\theta} = \frac{n_1}{n_0}} \qquad (7\text{-}7)$$

Obviously, if this refracted ray is to suffer total internal reflection at the core-cladding interface, the angle of incidence ϕ must satisfy the equation,

$$\boxed{\sin\phi (= \cos\theta) > \frac{n_2}{n_1}} \qquad (7\text{-}8)$$

Since $\sin\theta = \sqrt{1 - \cos^2\ \theta}$, we will have

$$\boxed{\sin\theta < \left[1 - \left(\frac{n_2}{n_1}\right)^2\right]^{1/2}} \qquad (7\text{-}9)$$

Let i_m represent the maximum half-angle of the acceptance cone for rays at the input end. Applying Snell's law at the input end and using Equations 7-5, 7-7, and 7-9, we must have $I < i_m$, where

$$\sin i_m = \left(n_1^2 - n_2^2\right)^{1/2} = n_1\sqrt{2\Delta} \tag{7-10}$$

and we have assumed $n_0 = 1$; i.e., the outside medium is assumed to be air. Thus, if a cone of light is incident on one end of the fiber, it will be guided through it provided the half-angle of the cone is less than i_m . This half-angle is a measure of the light-gathering power of the fiber. We define the numerical aperture (*NA*)—see Module 1-3, *Basic Geometrical Optics*—of the fiber by the following equation:

$$NA = \sin i_m = \sqrt{n_1^2 - n_2^2} = n_1\sqrt{2\Delta} \tag{7-11}$$

Example 7-2

For a typical step-index (multimode) fiber with $n_1 \approx 1.45$ and $\Delta \approx 0.01$, we get

$$\sin i_m = n_1\sqrt{2\Delta} = 1.45\sqrt{2 \times (0.01)} = 0.205$$

so that $i_m \approx 12°$. Thus, all light entering the fiber must be within a cone of half-angle 12°.

In a short length of an optical fiber, if all rays between $i = 0$ and i_m are launched, the light coming out of the fiber will also appear as a cone of half-angle i_m emanating from the fiber end. If we now allow this beam to fall normally on a white paper and measure its diameter, we can easily calculate the *NA* of the fiber (Laboratory B, "*NA* of a multimode optical fiber").

VI. ATTENUATION IN OPTICAL FIBERS

Attenuation and pulse dispersion represent the two most important characteristics of an optical fiber that determine the information-carrying capacity of a fiber optic communication system. Obviously, the lower the attenuation (and similarly, the lower the dispersion) the greater can be the required repeater spacing and therefore the lower will be the cost of the communication system. Pulse dispersion will be discussed in the next section, while in this section we will discuss briefly the various attenuation mechanisms in an optical fiber.

The attenuation of an optical beam is usually measured in decibels (dB). If an input power P_1 results in an output power P_2, the power loss α in decibels is given by

$$\alpha \text{ (dB)} = 10 \log_{10} (P_1/P_2) \tag{7-12}$$

Thus, if the output power is only half the input power, the loss is $10 \log 2 \approx 3$ dB. Similarly, if the power reduction is by a factor of 100 or 10, the power loss is 20 dB or 10 dB respectively. If

96% of the light is transmitted through the fiber, the loss is about 0.18 dB. On the other hand, in a typical fiber amplifier, a power amplification of about 1000 represents a power gain of 30 dB.

Figure 7-10 shows the spectral dependence of fiber *attenuation* (i.e., *loss coefficient per unit length*) as a function of wavelength of a typical silica optical fiber. The losses are caused by various mechanisms such as Rayleigh scattering, absorption due to metallic impurities and water in the fiber, and intrinsic absorption by the silica molecule itself. The Rayleigh scattering loss varies as $1/\lambda_0^4$, i.e., shorter wavelengths scatter more than longer wavelengths. Here λ_0 represents the free space wavelength. This is why the loss coefficient decreases up to about 1550 nm. The two absorption peaks around 1240 nm and 1380 nm are primarily due to traces of OH^- ions and traces of metallic ions. For example, even 1 part per million (ppm) of iron can cause a loss of about 0.68 dB/km at 1100 nm. Similarly, a concentration of 1 ppm of OH^- ion can cause a loss of 4 dB/km at 1380 nm. This shows the level of purity that is required to achieve low-loss optical fibers. If these impurities are removed, the two absorption peaks will disappear. For $\lambda_0 > 1600$ nm the increase in the loss coefficient is due to the absorption of infrared light by silica molecules. This is an intrinsic property of silica, and no amount of purification can remove this infrared absorption tail.

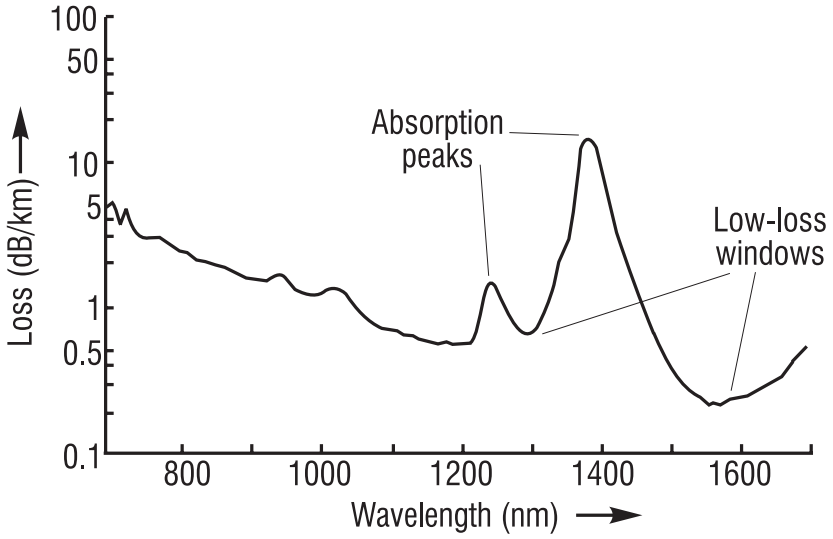

Figure 7-10 *Typical wavelength dependence of attenuation for a silica fiber. Notice that the lowest attenuation occurs at 1550 nm [adapted from Miya, Hasaka, and Miyashita].*

As you see, there are two windows at which loss attains its minimum value. The first window is around 1300 nm (with a typical loss coefficient of less than 1 dB/km) where, fortunately (as we will see later), the material dispersion is negligible. However, the loss attains its absolute minimum value of about 0.2 dB/km around 1550 nm. The latter window has become extremely important in view of the availability of erbium-doped fiber amplifiers.

Example 7-3

Calculation of losses using the dB scale become easy. For example, if we have a 40-km fiber link (with a loss of 0.4 dB/km) having 3 connectors in its path and if each connector has a loss of 1.8 dB, the total loss will be the sum of all the losses in dB; or 0.4 dB/km × 40 km + 3 × 1.8 dB = 21.4 dB.

Example 7-4

Let us assume that the input power of a 5-mW laser decreases to 30 μW after traversing through 40 km of an optical fiber. Using Equation 7-12, attenuation of the fiber in dB/km is therefore [10 log (166.7)]/40 ≈ 0.56 dB/km.

VII. PULSE DISPERSION IN STEP-INDEX FIBERS (SIF)

In digital communication systems, information to be sent is first coded in the form of pulses and these pulses of light are then transmitted from the transmitter to the receiver, where the information is decoded. The larger the number of pulses that can be sent per unit time and still be resolvable at the receiver end, the larger will be the transmission capacity of the system. A pulse of light sent into a fiber broadens in time as it propagates through the fiber. This phenomenon is known as *pulse dispersion,* and it occurs primarily because of the following mechanisms:

1. Different rays take different times to propagate through a given length of the fiber. We will discuss this for a step-index multimode fiber and for a parabolic-index fiber in this and the following sections. In the language of wave optics, this is known as *intermodal dispersion* because it arises due to different modes traveling with different speeds.[4]
2. Any given light source emits over a range of wavelengths, and, because of the intrinsic property of the material of the fiber, different wavelengths take different amounts of time to propagate along the same path. This is known as *material dispersion* and will be discussed in Section IX.
3. Apart from intermodal and material dispersions, there is yet another mechanism—referred to as *waveguide dispersion* and important only in single-mode fibers. We will briefly discuss this in Section XI.

In the fiber shown in Figure 7-7, the rays making larger angles with the axis (those shown as dotted rays) have to traverse a longer optical path length and therefore take a longer time to reach the output end. Consequently, the pulse broadens as it propagates through the fiber (see

[4] We will have a very brief discussion about modes in Section XI. We may mention here that the number of modes in a step index fiber is about $V^2/2$ where the parameter V will be defined in Section XI. When $V < 4$, the fiber supports only a few modes and it is necessary to use wave theory. On the other hand, if $V > 8$, the fiber supports many modes and the fiber is referred to as a multimoded fiber. When this happens, ray optics gives accurate results and one need not use wave theory.

Figure 7-11). Even though two pulses may be well resolved at the input end, because of the broadening of the pulses they may not be so at the output end. Where the output pulses are not resolvable, no information can be retrieved. Thus, the smaller the pulse dispersion, the greater will be the information-carrying capacity of the system.

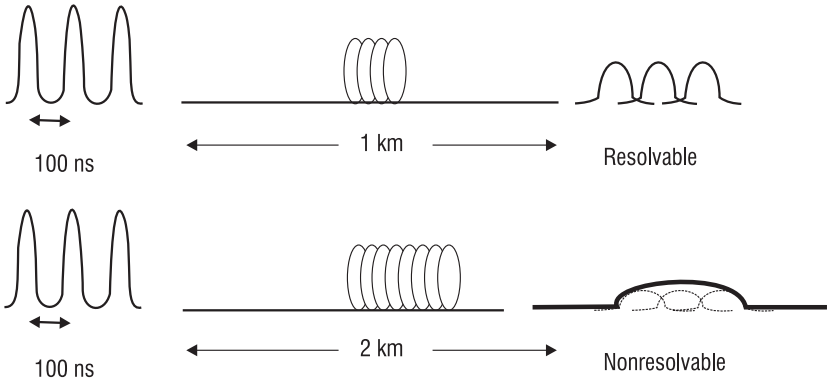

Figure 7-11 *Pulses separated by 100 ns at the input end would be resolvable at the output end of 1 km of the fiber. The same pulses would not be resolvable at the output end of 2 km of the same fiber.*

We will now derive an expression for the *intermodal dispersion* for a step-index fiber. Referring back to Figure 7-7b, for a ray making an angle θ with the axis, the distance *AB* is traversed in time.

$$t_{AB} = \frac{AC + CB}{c / n_1} = \frac{AB / \cos\theta}{c / n_1} \tag{7-13}$$

or

$$t_{AB} = \frac{n_{1(AB)}}{c\ cos\theta} \tag{7-14}$$

where c/n_1 represents the speed of light in a medium of refractive index n_1, c being the speed of light in free space. Since the ray path will repeat itself, the time taken by a ray to traverse a length L of the fiber would be

$$t_L = \frac{n_1 L}{c\ cos\theta} \tag{7-15}$$

The above expression shows that the time taken by a ray is a function of the angle θ made by the ray with the z-axis (fiber axis), which leads to pulse dispersion. If we assume that all rays lying between $\theta = 0$ and $\theta = \theta_c = \cos^{-1}(n_2/n_1)$ (see Equation 7-8) are present, the time taken by The following extreme rays for a fiber of length L would be given by

$$t_{\min} = \frac{n_1 L}{c} \qquad \text{corresponding to rays at } \theta = 0 \tag{7-16}$$

$$t_{\max} = \frac{n_1^2 L}{c n_2}$$ corresponding to rays at $\theta = \theta_c = \cos^{-1}(n_2/n_1)$ (7-17)

Hence, if all the input rays were excited simultaneously, the rays would occupy a time interval at the output end of duration

$$\tau_i = t_{\max} - t_{\min} = \frac{n_1 L}{c}\left[\frac{n_1}{n_2} - 1\right]$$

or, finally, the intermodal dispersion in a multimode SIF is

$$\tau_i \cong \frac{n_1 L}{c}\Delta \approx \frac{L}{2n_1 c}(NA)^2 \qquad (7\text{-}18)$$

where Δ has been defined earlier [see Equations 7-5 and 7-6] and we have used Equation 7-11. The quantity τ_i represents the pulse dispersion due to different rays taking different times in propagating through the fiber, which, in wave optics, is nothing but the intermodal dispersion and hence the subscript *i*. Note that the pulse dispersion is proportional to the square of *NA*. Thus, to have a smaller dispersion, one must have a smaller *NA*, which of course reduces the acceptance angle i_m and hence the light-gathering power. If, at the input end of the fiber, we have a pulse of width τ_1, after propagating through a length *L* of the fiber the pulse will have a width τ_2 given approximately by

$$\tau_2^2 = \tau_1^2 + \tau_i^2 \qquad (7\text{-}19)$$

Example 7-5

For a typical (multimoded) step-index fiber, if we assume $n_1 = 1.5$, $\Delta = 0.01$, $L = 1$ km, we would get

$$\tau_1 = \frac{1.5 \times 1000}{3 \times 10^8} \times 0.01 = 50 \text{ ns/km} \qquad (7\text{-}20)$$

That is, a pulse traversing through the fiber of length 1 km will be broadened by 50 ns. Thus, two pulses separated by, say, 500 ns at the input end will be quite resolvable at the end of 1 km of the fiber. However, if consecutive pulses were separated by, say, 10 ns at the input end, they would be absolutely unresolvable at the output end. Hence, in a 1-Mbit/s fiber optic system, where we have one pulse every 10^{-6} s, a 50-ns/km dispersion would require repeaters to be placed every 3 to 4 km. On the other hand, in a 1-Gbit/s fiber optic communication system, which requires the transmission of one pulse every 10^{-9}s, a dispersion of 50 ns/km would result in intolerable broadening even within 50 meters or so. This would be highly inefficient and uneconomical from a system point of view.

From the discussion in the above example it follows that, for a very-high-information-carrying system, it is necessary to reduce the pulse dispersion. Two alternative solutions exist—one involves the use of near-parabolic-index fibers and the other involves single-mode fibers. We look at these next.

VIII. PARABOLIC-INDEX FIBERS (PIF)

In a step-index fiber such as that pictured in Figure 7-7, the refractive index of the core has a constant value. By contrast, in a parabolic-index fiber, the refractive index in the core decreases continuously (in a quadratic fashion) from a maximum value at the center of the core to a constant value at the core-cladding interface. The refractive index variation is given by

$$\begin{aligned} n^2(r) &= n_1^2\left[1-2\Delta\left(\frac{r}{a}\right)^2\right] \qquad 0<r<a \quad \text{core} \\ n^2(r) &= n_2^2 = n_1^2(1-2\Delta) \qquad r>a \quad \text{cladding} \end{aligned} \tag{7-21}$$

with Δ as defined in Equation 7-5. For a typical (multimode) parabolic-index silica fiber, $\Delta \approx 0.01$, $n_2 \approx 1.45$, and $a \approx 25$ μm. On the other hand, for a typical plastic fiber (see Section XII), $n_1 \approx 1.49$, $n_2 \approx 1.40$, and $a \approx 500$ μm.

Since the refractive index decreases as one moves away from the center of the core, a ray entering the fiber is continuously bent toward the axis of the fiber, as depicted in Figure 7-12.

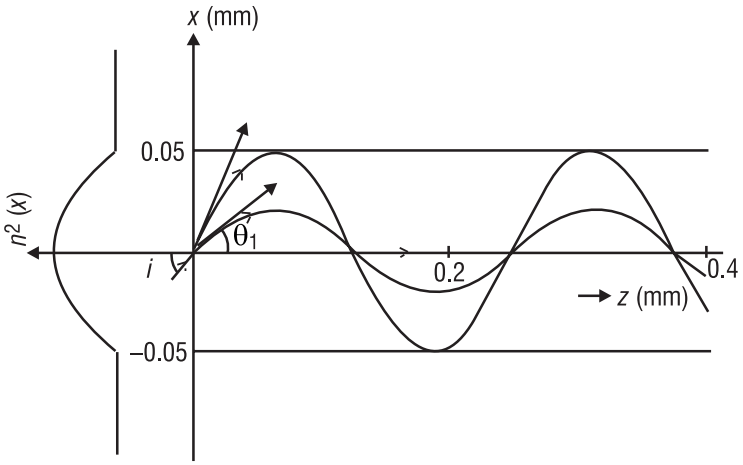

Figure 7-12 *Different ray paths in a parabolic-index fiber*

This follows from Snell's law because the ray continuously encounters a medium of lower refractive index and hence bends continuously away from the normal. Even though rays making larger angles with the fiber axis traverse a longer path, they do so now in a region of lower refractive index (and hence greater speed). The longer path length is almost compensated for by a greater average speed such that all rays take approximately the same amount of time in traversing the fiber. This leads to a much smaller pulse dispersion. The detailed calculations are

a bit involved [see, e.g., Chapters 4 and 5, Ghatak and Thyagarajan]. The final result for the intermodal dispersion in a parabolic-index fiber (PIF) is given by

$$\tau_{im} = \frac{n_2 L}{2c}\left(\frac{n_1 - n_2}{n_2}\right)^2 \approx \frac{n_2 L}{2c}\Delta^2 \approx \frac{L}{8cn_1^3}(NA)^4$$ Pulse dispersion in multimode PIF (7-22)

Note that, as compared to a step-index fiber, the pulse dispersion is proportional to the fourth power of *NA*. For a typical (multimode parabolic-index) fiber with $n_2 \approx 1.45$ and $\Delta \approx 0.01$, we would get

$$\tau_{im} \approx 0.25 \text{ ns/km}$$ (7-23)

Comparing with Equation 7-20 we find that for a parabolic-index fiber the pulse dispersion is reduced by a factor of about 200 in comparison to a step-index fiber. This is why first- and second-generation optical communication systems used near-parabolic-index fibers. To further decrease the pulse dispersion, it is necessary to use single-mode fibers, which will be discussed in Section XI. However, in all fiber optic systems we will have material dispersion (which is a characteristic of the material itself and not of the waveguide). We will discuss material dispersion in the following section.

IX. MATERIAL DISPERSION

We first define the *group index*. To do this we return to Equation 7-1 where we noted that the velocity of light in a medium is given by

$$v = c/n$$ (7-24)

Here *n* is the refractive index of the medium, which, in general, depends on the wavelength. The dependence of the refractive index on wavelength leads to what is known as *dispersion,* discussed in Module 1.3, *Basic Geometrical Optics*. In Figure 7-13 we have shown a narrow pencil of a white light beam incident on a prism. Since the refractive index of glass depends on the wavelength, the angle of refraction will be different for different colors. For example, for crown glass the refractive indices at 656.3 nm (orange), 589.0 nm (yellow), and 486.1 nm (green) are respectively given by 1.5244, 1.5270, and 1.5330. Thus, if the angle of incidence $i = 45°$ the angle of refraction, *r*, will be $r = 27.64°$, 27.58°, and 27.47° for the orange, yellow, and blue colors respectively. The incident white light will therefore *disperse* into its constituent colors—the dispersion will become more evident at the second surface of the prism as seen in Figure 7-13.

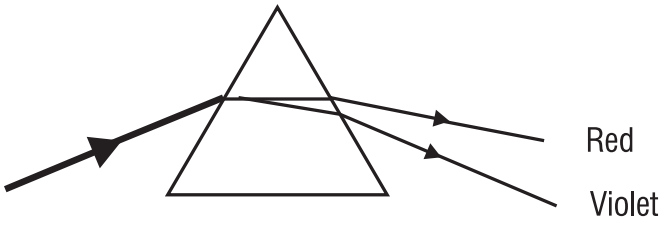

Figure 7-13 *Dispersion of white light as it passes through a prism*

Now, the quantity v defined by Equation 7-24 is usually referred to as the *phase velocity*. However, a pulse travels with what is known as the *group velocity,* which is given by

$$\boxed{v_g = c/n_g} \qquad (7\text{-}25)$$

where n_g is known as the group index and, in most cases its value is slightly larger than n. In Table 7.1 we have tabulated n and n_g for pure silica for different values of wavelength lying between 700 nm and 1600 nm. The corresponding spectral variation of n and n_g for pure silica is given in Figure 7-14.

Table 7.1 Values of n, n_g, and D_m for pure silica

λ_0 (nm)	n (λ_0)	n_g (λ_0)	D_m (ps/nm-km)
700	1.45561	1.47154	–172.902
750	1.45456	1.46924	–135.313
800	1.45364	1.46744	–106.609
850	1.45282	1.46601	–84.2077
900	1.45208	1.46489	–66.382
950	1.45139	1.46401	–51.9441
1000	1.45075	1.46332	–40.0577
1050	1.45013	1.46279	–30.1214
1100	1.44954	1.46241	–21.6951
1150	1.44896	1.46214	–14.4511
1200	1.44839	1.46197	–8.14213
1250	1.44783	1.46189	–2.57872
1300	1.44726	1.46189	2.38579
1350	1.44670	1.46196	6.86631
1400	1.44613	1.46209	10.9539
1450	1.44556	1.46229	14.7211
1500	1.44498	1.46253	18.2268
1550	1.44439	1.46283	21.5187
1600	1.44379	1.46318	24.6358

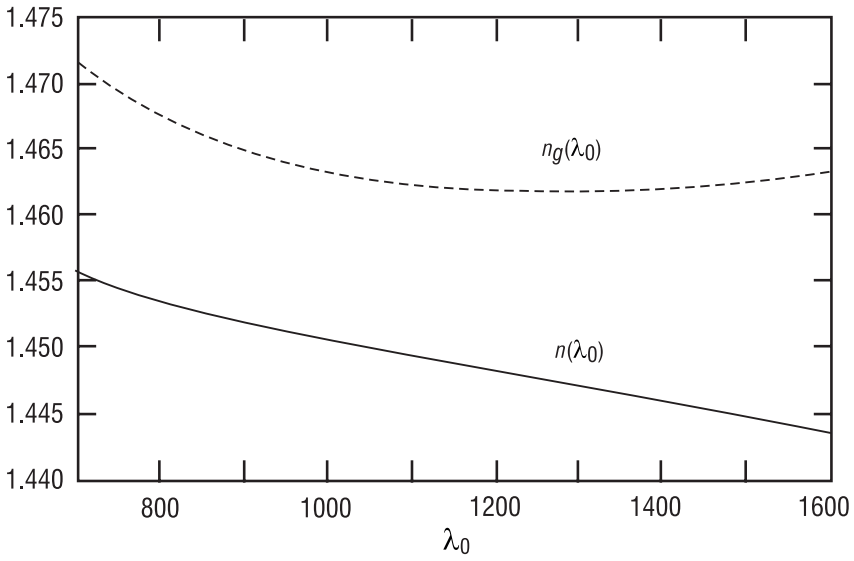

Figure 7-14 *Variation of* n *and* n_g *with wavelength for pure silica. Notice that* n_g *has a minimum value around 1270 nm.*

In Sections VIII and IX we considered the broadening of an optical pulse due to different rays taking different amounts of time to propagate through a certain length of the fiber. However, every source of light has a certain wavelength spread, which is often referred to as the spectral width of the source. Thus, a white light source (like the sun) has a spectral width of about 300 nm. On the other hand, an LED has a spectral width of about 25 nm and a typical laser diode (LD) operating at 1300 nm has a spectral width of about 2 nm or less. Each wavelength component will travel with a slightly different group velocity through the fiber. This results in broadening of a pulse. This broadening of the pulse is proportional to the length of the fiber and to the spectral width of the source. We define the *material dispersion coefficient* D_m, which is measured in ps/km-nm. D_m represents the material dispersion in picoseconds per kilometer length of the fiber per nanometer spectral width of the source. At a particular wavelength, the value of D_m is a characteristic of the material and is (almost) the same for *all* silica fibers. The values of D_m for different wavelengths are tabulated in Table 7.1. A negative D_m implies that the longer wavelengths travel faster; similarly, a positive value of D_m implies that shorter wavelengths travel faster. However, in calculating the pulse broadening, only the magnitude should be considered.

Example 7-6

The LEDs used in early optical communication systems had a spectral width $\Delta\lambda_0$ of about 20 nm around $\lambda_0 = 825$ nm. Using D_m in Table 7.1 (at 850 nm), such a pulse will broaden by

$$\tau_m = D_m \times L \times \Delta\lambda = 84.2 \text{ (ps/km-nm)} \times 1 \text{ (km)} \times 20 \text{ (nm)} \sim 1700 \text{ ps} = 1.7 \text{ ns}$$

in traversing a 1-km length of the fiber. It is very interesting to note that, if we carry out a similar calculation around $\lambda_0 \approx 1300$ nm, we will obtain a much smaller value of τ_m; thus

$$\tau_m = D_m \times L \times \Delta\lambda = 2.4 \text{ (ps/km-nm)} \times 1 \text{ (km)} \times 20 \text{ (nm)} \sim 0.05 \text{ ns}$$

in traversing 1-km length of the fiber. The very small value of τ_m is due to the fact that n_g is approximately constant around $\lambda_0 = 1300$ nm, as shown in Figure 7-14. Indeed, the wavelength $\lambda_0 \approx 1270$ nm is usually referred to as the zero material dispersion wavelength, and it is because of such low material dispersion that the optical communication systems shifted their operation to around $\lambda_0 \approx 1300$ nm.

Example 7-7

In the optical communication systems that are in operation today, one uses laser diodes (LD) with $\lambda_0 \approx 1550$ nm having a spectral width of about 2 nm. Thus, for a 1-km length of the fiber, the material dispersion τ_m becomes

$$\tau_m = D_m \times L \times \Delta\lambda = 21.5 \text{ (ps/km-nm)} \times 1 \text{ (km)} \times 2 \text{ (nm)} \sim 43 \text{ ps}$$

the positive sign indicating that higher wavelengths travel more slowly than lower wavelengths. [Notice from Table 7.1 that, for $\lambda_0 \geq 1300$ nm, n_g increases with λ_0.]

X. DISPERSION AND MAXIMUM BIT RATE

We may mention here briefly that, in a digital communication system employing light pulses, pulse broadening would result in an overlap of pulses, resulting in loss of resolution and leading to errors in detection. Thus pulse broadening is one of the mechanisms (other than attenuation) that limits the distance between two repeaters in a fiber optic link. It is obvious that, the larger the pulse broadening, the smaller will be the number of pulses per second that can be sent down a link. Different criteria based on slightly different considerations are used to estimate the maximum permissible bit rate (B_{max}) for a given pulse dispersion. However, it is always of the order of $1/\tau$, where τ is the pulse dispersion. In one type of extensively used coding (known as NRZ) we have

$$\boxed{B_{max} \approx 0.7/\tau} \qquad (7\text{-}26)$$

This formula takes into account (approximately) only the limitation imposed by the pulse dispersion in the fiber. In an actual link the source and detector characteristics would also be taken into account while estimating the maximum bit rate (see Module 1-8, *Fiber Optic Telecommunication*). It should also be pointed out that, in a fiber, the pulse dispersion is caused, in general, by intermodal dispersion, material dispersion, and waveguide dispersion. However, waveguide dispersion is important only in single-mode fibers and may be neglected in carrying out analysis for multimode fibers. Thus (considering multimode fibers), if τ_i and τ_m are the dispersion due to intermodal and material dispersions respectively, the total dispersion is given by

$$\boxed{\tau = \sqrt{\tau_i^2 + \tau_m^2}} \qquad (7\text{-}27)$$

Example 7-8

We consider a step-index multimode fiber with $n_1 = 1.46$, $\Delta = 0.01$, operating at 850 nm. For such a fiber, the intermodal dispersion (for a 1-km length) is

$$\tau_i = \frac{n_1 L \Delta}{c} \approx \frac{1.46 \times 1000 \times 0.01}{3 \times 10^8} \approx 49 \text{ ns}$$

which is usually written as

$$\tau_1 \approx 49 \text{ ns/km}$$

If the source is an LED with $\Delta\lambda = 20$ nm, using Table 7.1, the material dispersion τ_m is 1.7 ns/km [see Example 7-6]. Thus, in step-index multimode fibers, the dominant pulse-broadening mechanism is intermodal dispersion and the total dispersion is given by

$$\tau = \sqrt{\tau_i^2 + \tau_m^2} = 49 \text{ ns/km}$$

Using Equation 7-26, this gives a maximum bit rate of about

$$B_{\max} \approx 0.7/\tau \approx 14 \text{ Mbit-km/s}$$

Thus a 10-km link can at most support 1.4 Mbit/s, since τ increases by a factor of 10, causing $B_{\max}$ to decrease by the same factor.

Example 7-9

Let us now consider a parabolic-index multimode fiber with $n_1 = 1.46$, $\Delta = 0.01$, operating at 850 nm with an LED of spectral width 20 nm. For such a fiber, the intermodal dispersion, using Equation 7-22, is

$$\tau_{\text{im}} = \frac{n_1}{2c} \Delta^2 \text{L} \approx 0.24 \text{ ns/km}$$

The material dispersion is again 1.7 ns/km. Thus, in this case the dominant mechanism is material dispersion rather than intermodal dispersion. The total dispersion is

$$\tau = \sqrt{0.24^2 + 1.7^2} = 1.72 \text{ ns/km}$$

This gives a maximum bit rate of about

$$B_{\max} \approx 0.7/\tau \approx 400 \text{ Mbit-km/s}$$

giving a maximum permissible bit rate of 20 Mbit/s for a 20-km link.

Example 7-10

If we now shift the wavelength of operation to 1300 nm and use the parabolic-index fiber of the previous example, we see that the intermodal dispersion remains the same at 0.24 ns/km while the material dispersion (for an LED of $\Delta\lambda_0 = 20$ nm) becomes 0.05 ns/km (see Example 7-6). The

material dispersion is now negligible in comparison to intermodal dispersion. Thus the total dispersion and maximum bit rate are respectively given by

$$\tau \approx \sqrt{0.24^2 + 0.05^2} \approx 0.25 \text{ ns/km}; \Rightarrow B_{max} = 2.8 \text{ Gbit-km/s}$$

Example 7-11

If, in Example 7-10, we replace the LED with a laser diode of spectral width 2 nm, the material dispersion becomes 0.17 ns/km, which is now smaller than the intermodal dispersion. The total dispersion is

$$\tau = \sqrt{0.24^2 + 0.17^2} = 0.29 \text{ ns/km}$$

giving a maximum bit rate of

$$B_{max} = 0.7/\tau \approx 2.4 \text{ Gbit-km/s}$$

We should reiterate that, in the examples discussed above, the maximum bit rate has been estimated by considering the fiber only. In an actual link, the temporal response of the source and detector must also be taken into account.

XI. SINGLE-MODE FIBERS

While discussing step-index fibers, we considered light propagation inside the fiber as a set of many rays bouncing back and forth at the core-cladding interface (see Figure 7-7). There the angle θ could take a continuum of values lying between 0 and $\cos^{-1}(n_2/n_1)$, i.e.,

$$0 < \theta < \cos^{-1}(n_2/n_1)$$

For $n_2 = 1.5$ and $\Delta \approx \frac{n_1 - n_2}{n_1} = 0.01$, we would get $n_2/n_1 \simeq$ and $\cos^{-1}(\frac{n_2}{n_1}) = 8.1°$, so

$$0 < \theta < 8.1°$$

Now, when the core radius (or the quantity Δ) becomes very small, ray optics does not remain valid and one has to use the more accurate wave theory based on Maxwell's equations. This wave theory is fairly involved [see, e.g., Chapters 7 and 8 of Ghatak and Thyagarajan]. Here we just give some of the important results for a step-index fiber.

In wave theory, one introduces the parameter

$$V = \frac{2\pi}{\lambda_0} a\sqrt{n_1^2 - n_2^2} = \frac{2\pi}{\lambda_0} a n_1 \sqrt{2\Delta} \approx \frac{2\pi}{\lambda_0} a n_2 \sqrt{2\Delta} \qquad (7\text{-}28)$$

where Δ has been defined earlier (see Equation 7-5) and $n^1 \simeq n^2$. The quantity V is often referred to as the "*V-number*" or the "*waveguide parameter*" of the fiber. It can be shown that, if

$$V < 2.4045$$

only one guided mode (as if there is only one discrete value of θ) is possible and the fiber is known as a *single-mode fiber*. Further, for a step-index single-mode fiber, the corresponding (discrete) value of θ is approximately given by the following empirical formula

$$\cos\theta \approx 1 - \Delta\left[1 - \left(1.1428 - \frac{0.996}{V}\right)^2\right] \tag{7-29}$$

We may mention here that because of practical considerations the value of Δ ranges from about 0.002 to about 0.008.

Example 7-12

Consider a step-index fiber (operating at 1300 nm) with $n_2 = 1.447$, $\Delta = 0.003$, and $a = 4.2$ μm. Thus,

$$V = \frac{2\pi}{1.3(\mu\text{m})} \times 4.2(\mu\text{m}) \times 1.447 \times \sqrt{0.006} \approx 2.275$$

Thus the fiber will be single moded and the corresponding value of θ—using Equation 7-29—will be about $\theta = 3.1°$. It may be mentioned that for the given fiber we may write

$$V = \frac{2\pi}{\lambda_0(\mu\text{m})} \times 4.2(\mu\text{m}) \times 1.447 \times \sqrt{0.006} \approx \frac{2.958}{\lambda_0(\mu\text{m})}$$

Thus, for

$$\lambda_0 > 2.958/2.4045 = 1.23\ \mu\text{m}$$

which guarantees that $V < 2.4045$, the fiber will be single moded. The wavelength for which $V = 2.4045$ is known as the *cutoff wavelength* and is denoted by λ_c. In this example, $\lambda_c = 1.23$ μm and the fiber will be single moded for $\lambda_0 > 1.23$ μm.

Example 7-13

For reasons that will be discussed later, the fibers used in current optical communication systems (operating at 1.55 μm) have a small value of core radius and a large value of Δ. A typical fiber (operating at $\lambda_0 \approx 1.55$ μm) has $n_2 = 1.444$, $\Delta = 0.0075$, and $a = 2.3$ μm. Thus, at $\lambda_0 = 1.55$ μm, the V-number is,

$$V = \frac{2\pi}{1.55(\mu\text{m})} \times 2.3(\mu\text{m}) \times 1.444 \times \sqrt{0.015} \approx 1.649$$

The fiber will be single moded (at 1.55 μm) with $\theta = 5.9°$. Further, for the given fiber we may write

$$V = \frac{2\pi}{\lambda_0(\mu\text{m})} \times 2.3(\mu\text{m}) \times 1.444 \times \sqrt{0.015} \approx \frac{2.556}{\lambda_0(\mu\text{m})}$$

and therefore the cutoff wavelength will be $\lambda_c = 2.556/2.4045 = 1.06$ μm.

A. Spot size of the fundamental mode

A single-mode fiber supports only one mode that propagates through the fiber. This mode is also referred to as the *fundamental mode* of the fiber. The transverse field distribution associated with the fundamental mode of a single-mode fiber is an extremely important quantity. It determines various important parameters like splice loss at joints, launching efficiencies, bending loss, etc. For most single-mode fibers, the fundamental mode-field distributions can be approximated by a Gaussian function, which may be written in the form

$$\psi(r) = A \quad e^{-r^2/w^2} \tag{7-30}$$

where w is referred to as the spot size of the mode-field pattern. When $r = w$, the value of ψ is equal to $1/e$ of the value A at $r = 0$. For a step-index (single-mode) fiber, one has the following empirical expression for w [Marcuse]:

$$\frac{w}{a} \approx \left(0.65 + \frac{1.619}{V^{3/2}} + \frac{2.879}{V^6}\right); \qquad 0.8 < V < 2.5 \tag{7-31}$$

where a is the core radius and V is the V-number given by Equation 7-28. We may mention here that the light coming from a HeNe laser (or from a laser pointer) has a transverse intensity distribution very similar to that coming from a single-mode fiber except that the spot size for the HeNe laser is much larger. The quantity $2w$ is also referred to as the mode-field diameter (MFD) of the fiber and is a very important property of single-mode fibers. In fact, MFD is a more important property than core diameter in the case of single-mode fibers, since it determines the splice loss across a joint, bending loss, dispersion, etc. of single-mode fibers.

Example 7-14

Consider a step-index fiber (operating at 1300 nm) with $n_2 = 1.447$, $\Delta = 0.003$, and $a = 4.2$ μm. For this fiber (see Example 7-12), $V \approx 2.28$. Using Equation 7-31, with $V = 2.28$ and $a = 4.2$ mm, one obtains $w \approx 4.8$ μm. The same fiber will have a V-value of 1.908 at $\lambda_0 = 1550$ nm, giving a value of the spot size ≈ 5.5 μm. Thus the spot size increases with wavelength.

Example 7-15

For a step-index fiber (operating at 1550 nm) with $n_2 = 1.444$, $\Delta = 0.0075$, and $a = 2.3$ μm (see Example 7-13), $V \approx 1.65$, giving $w \approx 3.6$ μm. The same fiber will have a V-value of 1.97 at $\lambda_0 = 1300$ nm, giving a value of the spot size ≈ 3.0 μm.

B. Splice loss due to transverse misalignment

The most common misalignment at a joint between two similar fibers is the transverse misalignment similar to that shown in Figure 7-18. Corresponding to a transverse misalignment of *u,* the power loss in decibels is given by

$$\alpha\ (\text{dB}) \approx 4.34 \left(\frac{u}{w}\right)^2 \tag{7-32}$$

Thus a larger value of w will lead to a greater tolerance to transverse misalignment. For $w \approx 5$ μm, and a transverse offset of 1 μm, the loss at the joint will be approximately 0.18 dB. On the other hand, for $w \approx 3$ μm, a transverse offset of 1 μm will result in a loss of about 0.5 dB.

Example 7-16

Consider a single-mode fiber operating at 1300 nm with $w = 5$ μm. For the splice loss to be below 0.1 dB, we obtain [from Equation 7-32]

$$u < \sqrt{\alpha/4.34}\ w = \sqrt{0.1/4.34}\ (5\ \mu\text{m}) \approx 0.76\ \mu\text{m}$$

Thus we must have $u < 0.76$ μm. For a low-loss joint, the transverse alignment is very critical and connectors for single-mode fibers require precision matching and positioning for achieving low loss.

C. Waveguide dispersion

In Section IX we discussed material dispersion that results from the dependence of the refractive index of the fiber on wavelength. Even if we assume the refractive indices n_1 and n_2 to be independent of λ_0, the group velocity of each mode *does* depend on the wavelength. This leads to what is known as *waveguide dispersion*. The detailed theory is rather involved [see, e.g., Chapter 10, Ghatak and Thyagarajan]; we may mention here two important points:

1. The waveguide dispersion is usually negative for a given single-mode fiber. The magnitude increases with an increase in wavelength.
2. If the core radius a (of a single-mode fiber) is made smaller and the value of Δ is made larger, the magnitude of the waveguide dispersion increases. Thus we can tailor the waveguide dispersion by changing the refractive index profile.

The following two examples demonstrate how one can tailor the zero-dispersion wavelength by changing the fiber parameters.

Example 7-17

We consider the fiber discussed in Example 7-12 for which $n_2 = 1.447$, $\Delta = 0.003$, and $a = 4.2$ μm. The variations of the waveguide dispersion (τ_w), material dispersion (τ_m), and total dispersion

($\tau_{tot} = \tau_w + \tau_m$) with λ_0 are shown in Figure 7-15. From the figure it can be seen that the total dispersion passes through zero around $\lambda_0 \approx 1300$ nm. This is known as *zero total-dispersion wavelength* and represents an extremely important parameter.

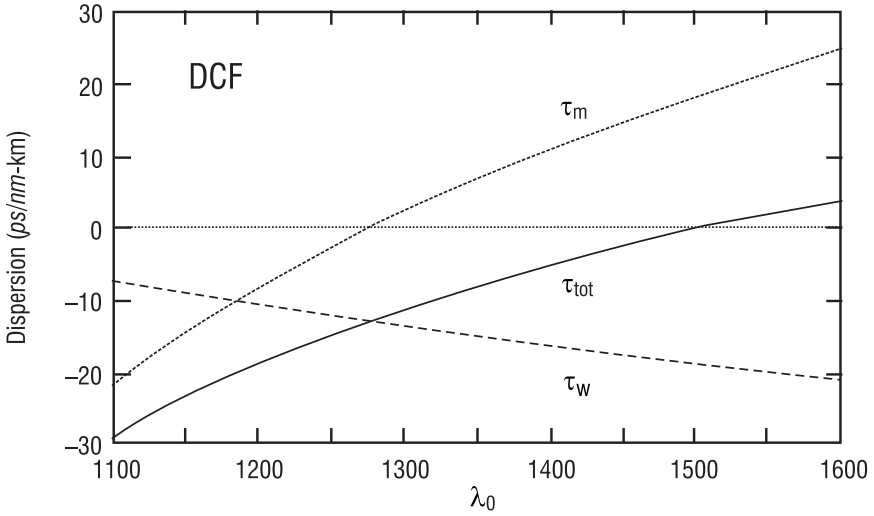

Figure 7-15 *The variations of τ_m, τ_w, and τ_{tot} with λ_0 for a typical conventional single-mode fiber (CSF) with parameters given in Example 7-17. The total dispersion passes through zero at around $\lambda_0 \approx 1300$ nm, known as* zero total dispersion wavelength.

Example 7-18

We next consider the fiber discussed in Example 7-13 for which $n_2 = 1.444$, $\Delta = 0.0075$, and $a = 2.3$ μm. For this fiber, at $\lambda_0 \approx 1550$ nm,

$\tau_w = -20$ ps/km-nm, as seen in Figure 7-16.

On the other hand, the material dispersion at this wavelength—per km and per unit wavelength interval in nm—is given by Table 7.1 as

$D_m = \tau_m = +21$ ps/km-nm

We therefore see that the two expressions are of opposite sign and almost cancel each other. Physically, because of waveguide dispersion, longer wavelengths travel more slowly than shorter wavelengths. And, because of material dispersion, longer wavelengths travel faster than shorter wavelengths. So the two effects compensate for each other, resulting in a zero total dispersion around 1550 nm. Thus we have been able to shift the zero-dispersion wavelength by changing the fiber parameters. These are known as the dispersion-shifted fibers, the importance of which will be discussed in the next section. The variations of τ_m, τ_w, and τ_{tot} with λ_0 are plotted in Figure 7-16, showing clearly that τ_{tot} is near zero at $\lambda_o = 1550$ nm.

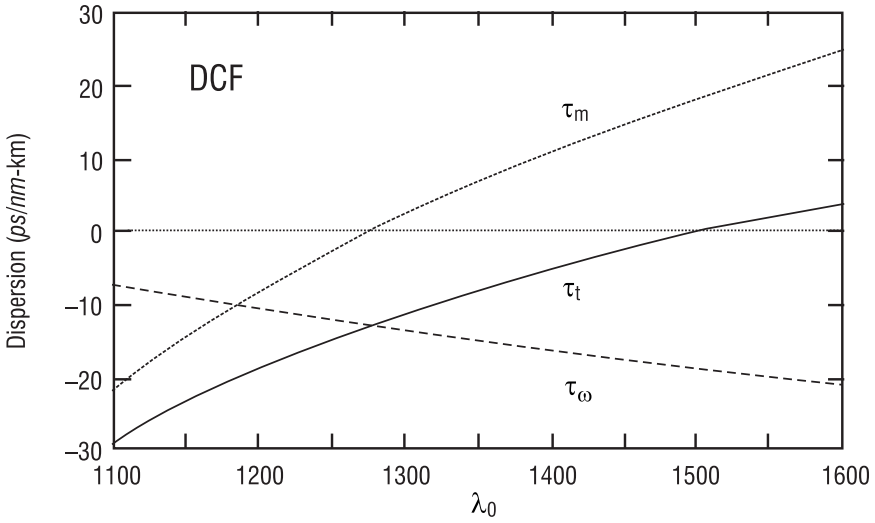

Figure 7-16 *The variations of τ_m, τ_w, and τ_{tot} with λ_0 for a typical dispersion-shifted single-mode fiber (DSF) with parameters given in Example 7-18. The total dispersion passes through zero at around $\lambda_0 \approx 1550$ nm.*

D. Dispersion-shifted fibers

In Section VI we learned that the attenuation of a silica fiber attains its minimum value of about 0.2 dB/km at around $\lambda_0 \approx 1550$ nm. The second- and third-generation optical communication systems operated around $\lambda_0 \approx 1300$ nm, where the dispersion was extremely small but the loss was about 1 dB/km, and therefore the repeater spacing was limited by the loss in the fiber. Since the lowest loss lies at around $\lambda_0 \approx 1550$ nm, if the zero-dispersion wavelength could be shifted to the $\lambda_0 \approx 1550$-nm region, one could have both minimum loss and very low dispersion. This would lead to very-high-bandwidth systems with very long (~ 100 km) repeater spacings. Apart from this, extremely efficient optical fiber amplifiers capable of amplifying optical signals in the 1550-nm band have also been developed. Thus, shifting the operating wavelength from 1310 nm to 1550 nm would be very advantageous. As discussed in Example 7-18, by reducing the core size and increasing the value of Δ, we can shift the zero-dispersion wavelength to 1550 nm, which represents the low-loss window. Indeed, the current fourth-generation optical communication systems operate at 1550 nm, using dispersion-shifted single-mode fibers with repeater spacing of about 100 km, carrying about 10 Gbit/s of information (equivalent to about 150,000 telephone channels) through one hair-thin single-mode fiber.

We may mention here that, if one is interested in carrying out accurate calculations for total dispersion, one may use the software described in Ghatak, Goyal, and Varshney.

XII. PLASTIC OPTICAL FIBERS (POF)

Plastic optical fibers made from plastic materials such as polymethyl methacrylate PMMA ($n = 1.49$), polystyrene ($n = 1.59$), polycarbonates ($n = 1.5$–1.57), fluorinated polymers, and so on. These fibers share the advantages of glass optical fibers in terms of insensitivity to electromagnetic interference, small size and weight, low cost, and potential capability of

carrying information at high rates. The most important attribute of POFs is their large core diameters of around 1 mm as compared to glass fibers with cores of 50 μm or 62.5 μm. Such a large diameter results in easier alignment at joints. They are also more durable and flexible than glass fibers. In addition, they usually have a large *NA*, resulting in larger light-gathering power (see Section VI).

Plastic optical fibers' performance lies somewhere between conventional copper wires and glass optical fibers. Copper wires are expensive and suffer from electromagnetic interference. By comparison, plastic optical fibers are cheaper and are free from interference. In addition, signals through copper wires can be tapped while it is very difficult to tap signals from optical fibers. Compared to glass fibers, POFs are much easier to connect because of their large diameters. Coupling of light from a source is also very efficient due to large *NA* and large core diameter. Thus, although glass optical fibers dominate long-distance data communication, POFs are expected to provide *low-cost solutions to short-distance applications* such as local area networks (LAN) and high-speed Internet access. At gigabit rates of transmission, glass fibers are at least 30% more expensive than POFs, while the cost of copper increases dramatically.

Attenuation is one of the important parameters of an optical fiber. Figure 7-17 shows typical loss spectra of 1-mm-diameter step-index (SI) and graded-index (GI) PMMA-based POF. There are three low-loss windows, at 570 nm, 650 nm, and 780 nm. The loss of SI POF at the 650-nm window is about 110 dB/km. This is, of course, very large compared to silica fibers, which have typical losses of about a few dB/km in this wavelength region. The large losses are due to Rayleigh scattering, intrinsic absorption of the material itself, and impurities and absorption due to vibrational modes of the molecules. Because of the high losses, these fibers are used in only short-distance (~ a few hundred meters) communication links.

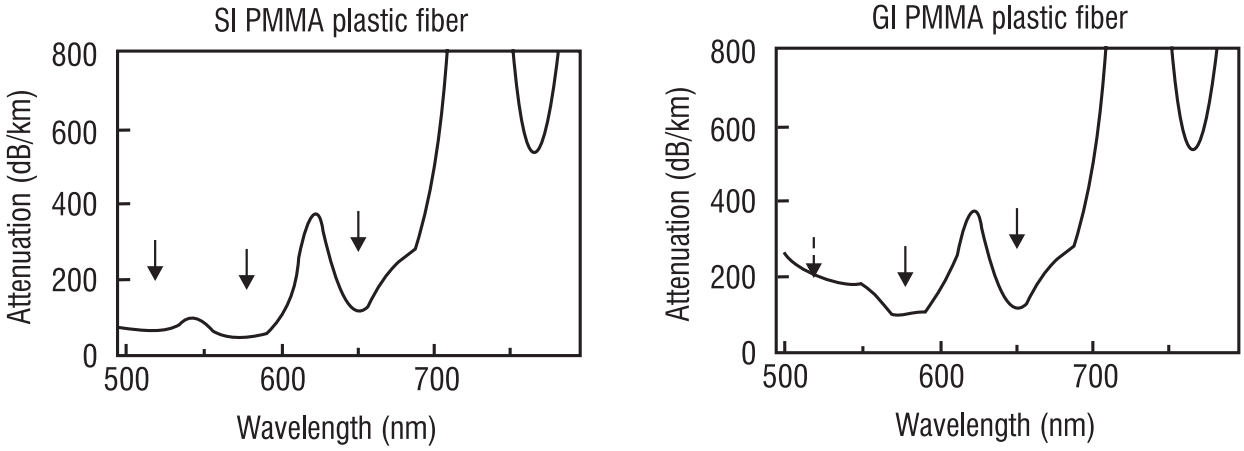

Figure 7-17 *Typical attenuation spectra of 1-mm-diameter (a) step-index (SI) and (b) graded-index (GI) PMMA plastic fiber [Adapted from Koeppen, Shi, Chen, and Garito]*

Example 7-19

An SI PMMA fiber has a core index of 1.49 and a cladding index of 1.40. Thus the *NA* [from Equation 7-11] is 0.51 giving an acceptance angle [from Equation. 7-11] of 31°. For such a POF, since the value of Δ (in this case ~ 0.06) is not very small, we must use Equation 7-5 and not the approximate expression given by Equation 7-6.

Example 7-20

The coupling efficiency η of light from an LED of an emitting area of radius a_s to a step-index optical fiber of core radius a is given [Keiser] as

$$\begin{cases} \eta = (NA)^2 & \text{for } a > a_s \\ \eta = \left(\dfrac{a}{a_s}\right)^2 (NA)^2 & \text{for } a < a_s \end{cases} \tag{7-33}$$

Thus, if the LED has an emitting radius of 35 μm and the fiber has an *NA* of 0.51 with a core diameter of 1 mm, the coupling efficiency [using the first part of Equation 7-33] will be about 25%. If the total power emitted by the LED is 10 mW, the power coupled will be 2.5 mW. For a typical step-index multimode glass optical fiber with $a \approx 25$ μm and $NA \approx 0.2$, the corresponding efficiency will be—using the second equation above—about 2%, giving a coupled power of 0.2 mW.

Example 7-21

Any transverse misalignment between the two cores across a joint between two fibers leads to a loss. The efficiency of coupling across a transverse misalignment between two step-index multimode fibers [Keiser] is given by Equation 7-34,

$$\eta = \frac{2}{\pi}\left\{\cos^{-1}\left(\tilde{d}\right) - \tilde{d}\left[1 - \left(\tilde{d}\right)^2\right]^{1/2}\right\}; \qquad \tilde{d} = \frac{d}{2a} \tag{7-34}$$

where d is the transverse separation between the cores of the two fibers and a is the core radius of the fibers. For misalignments of $d = 0.1\ a$ and $0.5\ a$, the efficiencies as given by the above equation are 94% and 69% respectively. For a 1-mm-diameter POF, these misalignments correspond to 50 μm and 250 μm respectively. For a glass fiber of radius 25 μm, these correspond to 2.5 μm and 12.5 μm respectively. This shows the much larger tolerance of POFs compared with glass silica fibers.

As discussed in Section VIII, pulse dispersion in multimode fibers can be reduced by using graded-index fibers with a near-parabolic refractive index variation in the core of the fiber.

Using various techniques, near-parabolic-index POFs have been fabricated (Koike, Ishigure, and Nihei). Such fibers can have very small pulse dispersion and hence can be used for high-bandwidth (~ hundreds of Mbit/s to Gbit/s) transmission over short lengths (~ 100 m). It is in fact the emergence of such a large-bandwidth graded-index plastic fiber that has spurred its use in many data-transfer applications.

Example 7-22

The coupling efficiency across a transverse misalignment of d between two identical parabolic-index fibers of radii a is given by (see, e. g., Keiser)

$$\eta = \frac{2}{\pi}\left\{\cos^{-1}\left(\tilde{d}\right) - \frac{\tilde{d}}{3}\left[1-\left(\tilde{d}\right)^2\right]^{1/2}(5-2\tilde{d}^2)\right\}; \qquad \tilde{d} = \frac{d}{2a} \tag{7-35}$$

We can approximate the above equation by $\eta \approx 1 - \frac{16\tilde{d}}{3\pi}$, which is accurate to within 1% for $\tilde{d} < 0.2$. Thus, for $d = 0.1a$ and $0.5a$, the coupling efficiencies would be about 91% and 59% respectively.

Example 7-23

Consider a step-index POF with core and cladding refractive indices given by 1.58 and 1.39 respectively. Using Equation 7-18 for the pulse dispersion in a step-index optical fiber, we obtain a pulse dispersion of 720 ns/km. For a link 100 m long, the dispersion would be 72 ns.

Example 7-24

Consider a parabolic-index POF with $n_1 = 1.490$ and $n_2 = 1.475$ (implying $NA \sim 0.21$ on the axis). We will calculate the pulse dispersion caused by intermodal dispersion only. Using Equation 7-22 we obtain the pulse dispersion as 0.25 ns/km. For a 100-m-long link, the intermodal dispersion would be 25 ps. In addition to the intermodal dispersion, the actual dispersion in such parabolic-index fibers would be determined by material dispersion and also by any mode-coupling effects that may take place in the fiber. In Koike, Ishigure, and Nihei, measurements have shown about 3-GHz bandwidth of graded-index POFs.

Example 7-25

The material dispersion of PMMA is about 0.305 ns/nm-km at 650 nm (Ishigure, Nihei, and Koike). If an LED source with a spectral width of 20 nm is used with a PMMA optical fiber, the material dispersion of the fiber will be $0.305 \times 20 = 6.1$ ns/km. If the spectral width of the source is reduced to 1 nm, the material dispersion reduces to 0.305 ns/km. In the presence of both intermodal and material dispersion, the total dispersion is given by Equation 7-27. Thus, if the intermodal dispersion of the fiber is 0.25 ns/km, the total dispersion for the two spectral widths is given by 6.1 ns/km and 0.394 ns/km respectively. For a 100-m-long fiber, the total dispersions are 0.61 ns and 0.039 ns. Thus, using Equation 7-38, the above dispersion values correspond to maximum bit rates of about 1.1 Gbit/s and 18 Gbit/s respectively using the NRZ scheme. This example shows the importance of reduced spectral width and use of graded-index fibers for achieving high-data-rate communication.

Apart from short-distance communication applications, POFs are expected to find applications in many areas such as lighting for decorative signs and road signs, or in museums (where the property of fibers in non-UV transmission is very useful), in image transmission as in endoscopes, and in sensing applications.

There is also interest in fluorescent or scintillating fibers, which are ordinary plastic fibers doped with special elements. When light falls on a fluorescent fiber, it excites the dopants in the fiber. When the atoms drop to a lower energy state, they emit light. Part of this light is collected within the fiber *NA* and is transmitted to both ends of the fiber. In scintillating fibers, light is generated when radiations such as α and β particles, or γ rays, are incident on the fiber. Many applications are being envisaged for fluorescent fibers, particularly due to their ability to capture light that falls anywhere along the length of the fiber. Applications include intrusion alarms and size determination. Scintillating optical fibers find applications in particle energy measurement, track detection, etc. For further details, readers may see Spillman and Gravel.

Example 7-26

Polycarbonate fibers with a core index of 1.58 and cladding index of 1.39 are available from some vendors. The *NA* of such fibers is 0.75, giving an acceptance angle of 49^{o}. Such large-*NA* fibers provide a large coupling efficiency from light source to fiber.

XIII. FIBER OPTIC SENSORS

Although the most important application of optical fibers is in the field of transmission of information, optical fibers capable of sensing various physical parameters and generating information are also finding widespread use. The use of optical fibers for such applications offers the same advantages as in the field of communication: lower cost, smaller size, more accuracy, greater flexibility, and greater reliability. As compared to conventional electrical sensors, fiber optic sensors are immune to external electromagnetic interference and can be used

in hazardous and explosive environments. A very important attribute of fiber optic sensors is the possibility of having distributed or quasi-distributed sensing geometries, which would otherwise be too expensive or complicated using conventional sensors. With fiber optic sensors it is possible to measure pressure, temperature, electric current, rotation, strain, and chemical and biological parameters with greater precision and speed. These advantages are leading to increased integration of such sensors in civil structures such as bridges and tunnels, process industries, medical instruments, aircraft, missiles, and even cars.

Fiber optic sensors can be broadly classified into two categories: *extrinsic* and *intrinsic*. In the case of extrinsic sensors, the optical fiber simply acts as a device to transmit and collect light from a sensing element, which is external to the fiber. The sensing element responds to the external perturbation, and the change in the characteristics of the sensing element is transmitted by the return fiber for analysis. The optical fiber here plays no role other than that of transmitting the light beam. On the other hand, in the case of intrinsic sensors, the physical parameter to be sensed directly alters the properties of the optical fiber, which in turn leads to changes in a characteristic such as intensity, polarization, or phase of the light beam propagating in the fiber.

A large variety of fiber optic sensors has been demonstrated in the laboratory, and some are already being installed in real systems. In the following, we will discuss some important examples of fiber optic sensors.

A. Extrinsic fiber optic sensors

Figure 7-18 shows a very simple sensor based on the fact that transmission through a fiber joint depends on the alignment of the fiber cores [see Equations 7-33 and 7-34]. Light coupled into a multimode optical fiber couples across a joint into another fiber. The light is detected by a photodetector. Any deviation of the fiber pair from perfect alignment is immediately sensed by the detector. A misalignment of magnitude equal to the core diameter of the fiber results in zero transmission. The first 20% of transverse displacement gives an approximately linear output. Thus, for a 50-μm-core-diameter fiber, approximately 10-μm misalignment will be linear. The sensitivity will of course become better with decrease in core diameter, but, at the same time, the range of displacements will also reduce.

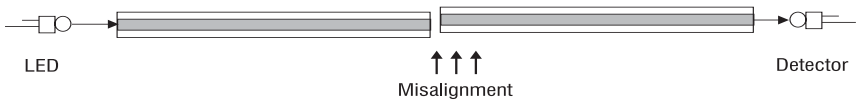

Figure 7-18 *A change in the transverse alignment between two fibers changes the coupling and hence the power falling on the detector.*

The misalignment between the fibers could be caused by various physical parameters, such as acoustic waves and pressure. Thus, if one of the probe fibers has a short free length while the other has a longer length, acoustic waves impinging on the sensor will set the fibers into vibration, which will result in a modulation of the transmitted light intensity leading to an acoustic sensor. Using such an arrangement, deep-sea noise levels in the frequency range of 100 Hz to 1 kHz and transverse displacements of a few tenths of a nanometer have been

measured (Spillman and Gravel). Using the same principle, any physical parameter leading to a relative displacement of the fiber cores can be sensed using this geometry.

Figure 7-19 shows a modification of the sensor in the form of a probe. Here light from an LED coupled into a multimode fiber passes through a fiber optic splitter to the probe. The probe is in the form of a reflecting diaphragm in front of the fiber, as shown. Light emanating from the fiber is reflected by the diaphragm, passes again through the splitter, and is detected by a photodetector. Any change in the external pressure causes the diaphragm to bend, leading to a change in the power coupled into the fiber. Such sensors can be built to measure pressure variations in medical as well as other applications requiring monitoring operating pressures of up to 4 mega Pascal (~ 600 psi) (Farmer and Digges). Such a device can be used for the measurement of pressure in the arteries, bladder, urethra, etc. Several experiments have shown a very good correlation between this sensor and other conventional sensors.

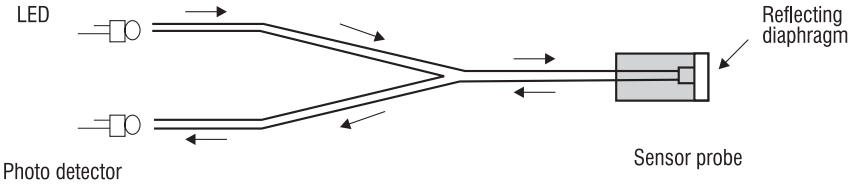

Figure 7-19 *Light returning to the detector changes as the shape of the reflecting diaphragm changes due to changes in external pressure.*

If the diaphragm at the output is removed and the light beam is allowed to fall on the sample, light that is reflected or scattered is again picked up by the fiber and detected and processed by the detector. With analysis of the returning optical beam, information about the physical and chemical properties of the blood can be obtained. Thus, if the scattering takes place from flowing blood, the scattered light beam is shifted in frequency due to the Doppler effect. (Doppler effect refers to the apparent frequency shift of a wave detected by an observer—compared with its true frequency—when there is relative motion between source and observer. You must have noticed the falling frequency of the whistle of a train as it approaches and recedes from you.). The faster the blood cells are moving, the larger will be the shift. Through measurement of the shift in frequency, the blood flow rate can be estimated. By a spectroscopic analysis of the returning optical signal, one can estimate the oxygen content in the blood. One of the most important advantages of using optical fibers in this process is that they do not provoke adverse response from the immune system. They are more durable, more flexible, and potentially safer than alternatives (Katzir, Grifford, and Bartnik).

Another very interesting sensor is the liquid-level sensor shown in Figure 7-20. Light propagating down an optical fiber is total internally reflected from a small glass prism and couples back to the return fiber. As long as the external medium is air, the angle of incidence inside the prism is greater than the critical angle and hence light suffers total internal reflection. As soon as the prism comes in contact with a liquid, the critical angle at the prism-liquid interface reduces and the light is transmitted into the liquid, resulting in a loss of signal. By a proper choice of prism material, such a sensor can be used for sensing levels of various liquids such as water, gasoline, acids, and oils.

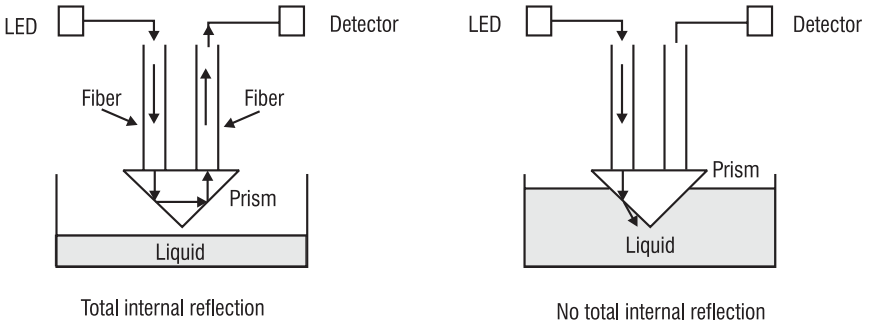

Figure 7-20 *A liquid-level sensor based on changes in the critical angle due to liquid level moving up to contact the sides of the prism*

Example 7-27

For a prism with refractive index n_p of 1.5, the critical angles with air ($n_a = 1.0$) and water ($n_w = 1.33$) are 41.8° and 62.7° respectively [see Example 7-1]. Thus, if the prism is isosceles right-angled, with two angles as 45°, light that suffers total internal reflection with air as the surrounding medium will suffer only partial internal reflection with water as the surrounding medium, resulting in a loss of signal.

B. Intrinsic sensors

In intrinsic sensors the physical parameter changes some characteristic of the propagating light beam that is sensed. Among the many intrinsic sensors, here we discuss two important examples, namely the Mach-Zehnder interferometric fiber sensor and the fiber optic gyroscope.

Mach-Zehnder interferometric sensor

One of the most sensitive arrangements for a fiber optic sensor is the Mach-Zehnder (MZ) interferometric sensor arrangement shown in Figure 7-21. Light from a laser is passed through a 3-dB fiber optic coupler, which splits the incoming light beam into two equal-amplitude beams in the two single-mode fiber arms. The light beams recombine at the output coupler after passing through the two arms. The output from the output coupler is detected and processed. One of the fiber arms of the interferometer is the sensing arm, which is sensitive to the external parameter to be sensed. The other fiber arm is the reference arm. It is usually coated with a material to make it insensitive to the parameter of measurement. The two fiber arms behave as two paths of an interferometer, and hence the output depends on the phase difference between the beams as they enter the output coupler. If the two fibers are of exactly equal lengths, the entire input light beam appears in the lower fiber and no light comes out of the upper fiber. Any external parameter such as temperature or pressure affects the sensing fiber by changing either the refractive index or the length of the arm, thus changing the phase difference between the two beams as they enter the output coupler. This results in a change in the intensity of the two output arms. Processing of the output leads to a measurement of the external parameter.

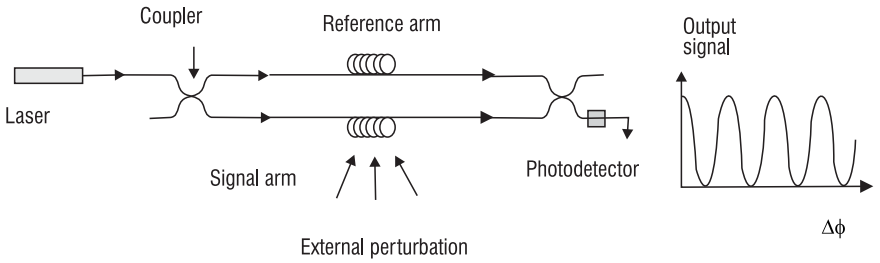

Figure 7-21 *The fiber optic Mach-Zehnder interferometric sensor. Phase changes (due to external perturbation on the sensing arm) between the light beams arriving at the output coupler cause changes in intensity at the output.*

The MZ sensor is extremely sensitive to external perturbations. For example, the change of phase due to an external pressure that causes both a change in refractive index and a change in the length of the specially coated sensing arm is about 3×10^{-4} rad/Pa-m. Here Pa = 1 N/m^2 represents a Pascal, the unit of pressure. This implies that the change of phase suffered by the beam when the external pressure changes by 1 Pa over 1 m of the fiber is 3×10^{-4}. When someone whispers, the sound pressure corresponds to about 2×10^{-4} Pa at a distance of 1 m. If the length of the sensing arm is 100 m, the corresponding phase change in the light propagating through the sensing arm is 6×10^{-6} rad. Such small changes in phase are detectable by sensitive signal processing.

MZ sensors can be used to sense different physical parameters such as temperature, strain, and magnetic field. These physical parameters cause changes in the phase of the propagating light beam. Such sensors are finding various applications in hydrophones for underwater sound detection. One of the great advantages of such an application is the possibility of configuring the sensors as omnidirectional or highly directional sensors.

Fiber optic rotation sensor—the fiber optic gyroscope (FOG)

One of the more important fiber optic sensors is the *fiber optic gyroscope*, capable of measuring rotation rate. The FOG is a device with no moving parts, with improved lifetime, and of relatively low cost. Thus FOGs are rapidly replacing conventional mechanical gyros for many applications.

The principle of operation of the fiber optic gyroscope is based on the *Sagnac effect*. Figure 7-22 shows a simple FOG configuration. It consists of a loop of polarization-maintaining, single-mode optical fiber connected to a pair of 3-dB directional couplers (capable of splitting the incoming light beam into two equal parts or combining the beams from both input fibers), a polarized source, and a detector. Light from the source is split into two equal parts at the coupler C_1, one part traveling clockwise and the other counterclockwise in the fiber coil. After traversing the coil the two light beams are recombined at the same coupler and the resulting light energy is detected by a photodetector connected to the coupler C_2. The source in a FOG is usually a source with a broad spectrum and hence a short coherence length. The source is chosen to avoid any coherent interference between backscattered light from the two counterpropagating beams in the fiber loop. This could be a superluminescent diode or a superfluorescent fiber source.

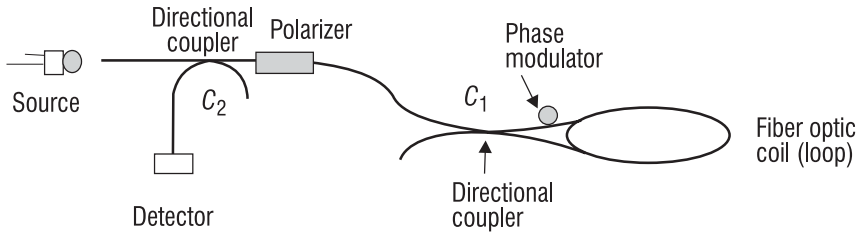

Figure 7-22 *A fiber optic gyroscope for rotation sensing based on the Sagnac effect*

We first note that, if the loop is not rotating, the clockwise and the counterclockwise beams will take the same time to traverse the loop and hence arrive at the same time with the same phase at the coupler C_1. On the other hand, when the loop begins to rotate, the times taken by the two beams are different. This can be understood from the fact that, if the loop rotates clockwise, by the time the beams traverse the loop the starting point will have moved and the clockwise beam will take a slightly longer time than the counterclockwise beam to come back to the starting point. This difference of time or phase will result in a change of intensity at the output light beam propagating toward C_2.

One of the great advantages of a Sagnac interferometer is that the sensor gives no signal for reciprocal stimuli, i.e., stimuli that *act in an identical fashion* on both the beams. Thus a change of temperature affects both the beams (clockwise and counterclockwise) equally and so produces no change in the output.

If the entire loop arrangement rotates with an angular velocity Ω, the phase difference between the two beams is given by

$$\boxed{\Delta\phi = \frac{8\pi NA\Omega}{c\lambda_0}} \qquad (7\text{-}36)$$

where N is the number of fiber turns in the loop

A is the area enclosed by one turn (which need not be circular)

λ_0 is the free space wavelength of light

Example 7-28

Let us consider a fiber optic gyroscope with a coil of diameter 10 cm, having 1500 turns (corresponding to a total fiber length of $\pi DN \sim 470$ m) and operating at 850 nm. The corresponding phase difference, determined from Equation 7-36 is $\Delta\phi = 1.16\ \Omega$ rad. If Ω corresponds to the rotation rate of the Earth (15° per hour) the corresponding phase shift is $\Delta\phi = 8.4 \times 10^{-5}$ rad, a small shift indeed. This phase difference corresponds to a flight time difference between the two beams of $\Delta\tau = \Delta\phi/\omega = \Delta\phi\ \lambda_0/(2\pi c) \approx 3.8 \times 10^{-20}$ s.

There are many different ways of operating the gyroscope. One of them is called the closed-loop operation. In this method, a pseudo rotation signal is generated in the gyro to cancel the actual signal caused due to the rotation, thus nulling the output. This is achieved by having a phase

modulator near one end of the loop as shown in Figure 7-22. The counterclockwise-traveling beam encounters the phase modulator later than the clockwise beam. This time difference introduces an artificial phase difference between the two beams. The applied signal on the modulator required to null the signal gives the rotation rate.

Fiber optic gyros capable of measuring from 0.001 deg/h to 100 deg/h are being made. Applications include navigation of aircraft, spacecraft, missiles, manned and unmanned platforms, antenna piloting and tracking, and a compass or north finder. Various applications require FOGs with different sensitivities: Autos require about 10 to 100 deg/h, attitude reference for airplanes requires 1 deg/h, and precision inertial navigation requires gyros with 0.01 to 0.001 deg/h. A Boeing 777 uses an inertial navigation system that has both ring laser gyroscopes and FOGs.

An interesting application involves automobile navigation. The autogyro provides information about the direction and distance traveled and the vehicle's location, which is shown on the monitor in the car. Thus the driver can navigate through a city. Luxury cars from Toyota and Nissan sold in Japan have FOGs as part of their on-board navigation systems. The biggest manufacturer of such gyros is Hitachi of Japan, which manufactures about 3000 gyros per month. [Burns. Bennet. Hotate]

Laboratory

Using the concepts developed in this module, you will be able to perform the following simple experimental projects as part of the laboratory exercise for this module.

- Differentiate between a multimode and a single-mode optical fiber
- Measure *NA* of a multimode optical fiber
- Measure the attenuation coefficient of a multimode optical fiber
- Determine the mode-field diameter (MFD) of a single-mode fiber
- Determine the splice loss across a multimode fiber joint

Equipment List

HeNe laser

Laser pointer

Multimode and single-mode optical fibers

Microscope objective (20X)

Optical power meter

Translational stages with micromovements (*xyz*-stack)

Fiber holders (V-groove)

Each of the projects identified above is described in detail below.

A. *Multimode and single-mode optical fibers*

Take 2-m lengths of multimode and single-mode optical fibers with cutoff wavelength less than 630 nm, so that the fibers are single moded at the HeNe laser wavelength of 633 nm. Couple light into the fibers and observe the output light as it falls on a screen. You should notice that the output from the multimode fiber is characterized by a speckle pattern while that of a single-mode fiber is uniform.

B. NA *of a multimode optical fiber*

Draw several concentric circles of increasing radii—say, from 0.5 cm to 1.5 cm—on a small paper screen. The screen is positioned in the far field (see Module 1-4, *Basic Physical Optics*) so that the axis of the fiber, at the output end, passes perpendicularly through the center of these circles on the screen (see Figure 7-23). The fiber end, which is mounted on an *xyz*-stack, is moved slightly toward or away from the screen so that one of the circles there just circumscribes the far-field radiation spot. The distance z between the fiber end and the screen, and the diameter D of the coinciding circle are measured accurately. The NA is calculated using the following equation

$$NA = \sin i_m = \sin\left[\tan^{-1}\left(D/2z\right)\right] \tag{7-37}$$

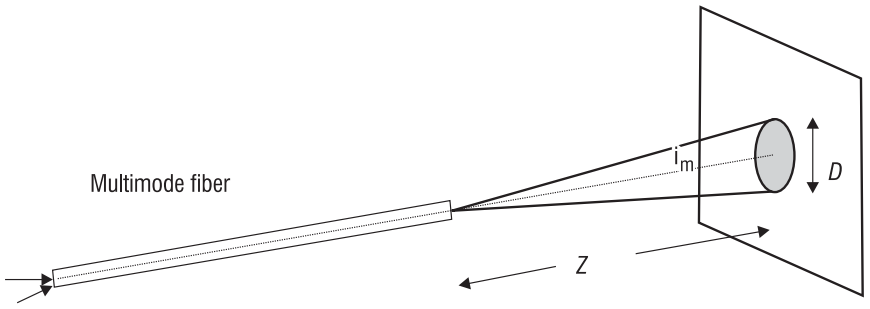

Figure 7-23 *Measurement of the diameter* D *of the spot on a screen placed at a far-field distance* z *from the output end of a multimode fiber can be used to measure the* NA *of the fiber.*

C. *Attenuation measurement*

A simple experiment can be performed for measuring the attenuation of the fiber at one specific wavelength. Take a length L (about 1 km) of the fiber and couple the beam from a laser into the fiber. Measure the power P_o exiting at the output end of the fiber. Without disturbing the coupling system, cut off a reference length of 1 m of the fiber from the input end. Measure the power P_i exiting from the 1-m length of the fiber. This will be the input power to the longer portion of the fiber. The attenuation coefficient of the fiber at the wavelength of the laser is then given by

$$\alpha \approx \frac{1}{L}\log\left(\frac{P_i}{P_o}\right) \text{ dB/km}$$

D. *MFD measurement of an SMF*

The MFD of a single-mode fiber can be easily determined by a measurement of the far-field radiation pattern emerging from the fiber. We have seen that the transverse field distribution of a single-mode fiber is approximately Gaussian in shape. When light exits the single-mode fiber, it diffracts as it propagates through air. The angle of diffraction is given approximately by

$$\theta \approx \frac{\lambda}{\pi w} \tag{7-38}$$

Thus a measurement of θ at a specific chosen wavelength in the single-mode regime can give us the value of *w*.

To perform the experiment, take a 2-m length of a single-mode fiber, preferably at a visible wavelength such as 633 nm (HeNe laser). Couple light into the fiber using a microscope objective of magnification 20X. Place the photodetector (covered by a pinhole of about 0.1-mm diameter) of an optical power meter at a distance *D* of about 10 cm from the output end of the fiber. Adjust the detector to coincide with the center of the radiation pattern by maximizing the power. Note the power. Move the photodetector so that the power drops to about $1/e^2$ (~ 0.135) of the maximum. Measure the corresponding distance *d* moved from the center. Then

$$\theta \approx \frac{d}{D} \approx \frac{\lambda}{\pi w} \tag{7-39}$$

Thus MFD = 2*w* can be easily calculated from the measured values of *d* and *D*.

E. *Splice loss across a multimode fiber joint*

In Examples 7-21 and 7-22 we discussed the loss at a joint between a pair of step-index fibers and a pair of parabolic-index multimode fibers. A simple experiment to measure the variation of splice loss across a transverse misalignment can be performed and fitted using the formulas given. Take a multimode optical fiber of about 5-meter length and cut it into two almost equal pieces. Prepare the fiber ends by using a standard fiber cutter. Couple light from a white light source (such as a halogen lamp) into one of the fibers by focusing the light using a microscope objective. Place the other end of the fiber on a V-groove and couple this to the other fiber, which is placed on an *xyz*-stack. Bring the two ends of the fibers as close as possible—as shown in Figure 7-18—and adjust the transverse position of the fibers so that you couple the maximum amount of light. Now move the fiber in the transverse direction in steps of 10 μm and measure the power at each point. Measure the power exiting from the fiber end after removing the second fiber. Calculate the coupling efficiency (η) and plot as a function of the transverse misalignment. If you have knowledge of the fiber parameters, you can use Equations 7-33 and 7-34 to plot the theoretical variations and compare the experimentally measured variation with the theoretical plot. This experiment will show the sensitivity of the loss to transverse alignment of the two fibers. This is an important consideration while designing connectors for fibers.

A similar experiment can be carried out with single-mode fibers. However, you will need very precise movements to carry out the experiment, since single-mode fibers typically have mode-

field diameters of about 5 to 10 μm. You will have to use Equation 7-32 to carry out the corresponding theoretical analysis.

Problems

1. For a step-index multimode fiber, $n_1 = 1.5$ and $\Delta = 0.015$, calculate n_2, NA, and the maximum acceptance angle. (Answer: 1.477, 0.26, 15°)
2. Based on the previous problem, consider the same step-index fiber immersed in water of refractive index 1.33. Calculate the maximum acceptance angle.
3. The power of a 2-mW laser beam decreases to 15 μW after the beam traverses through 25 km of a single-mode optical fiber. Calculate the attenuation of the fiber. (Answer: 0.85 dB/km)
4. A 5-mW laser beam passes through a 26-km fiber of loss 0.2 dB/km. Calculate the power at the output end. (Answer: 1.5 mW)
5. Consider an SIF with $n_1 = 1.5$, $a = 40$ μm, and $\Delta = 0.015$, operating at 850 nm with a spectral width of 50 nm. a) Is this a single-mode fiber or a multimode fiber? b) Calculate the material dispersion, intermodal dispersion, and total pulse dispersion. [Answer: (b) 4.2 ns/km, 75 ns/km, 75.1 ns/km]
6. Based on the previous problem, consider a parabolic-index fiber with $n_1 = 1.5$, $a = 40$ μm, and $\Delta = 0.015$, operating at 850 nm with a spectral width of 50 nm. a) Is this a single-mode fiber or a multimode fiber? b) Calculate the material dispersion, intermodal dispersion, and total pulse dispersion. [Answer: (b) 4.2 ns/km, 0.6 ns/km, 4.2 ns/km]
7. Consider a single-mode fiber with $a = 3$ μm operating with a V-number of 2.3. Calculate the spot size of the fundamental mode. [Answer: 3.4 μm]
8. Consider the SIF given in Problem 5. Calculate the splice loss at a joint between two such identical fibers with transverse misalignments of 5, 10, and 15 μm. [Answer: 0.36 dB, 0.75 dB, 1.2 dB]

References

Bennet, S. “Fibre Optic gyro system keeps bus riders informed,” *Photonics Spectra*, August 1996, pp. 117–120.

Burns. W.K. “Fiber Optic Gyroscopes—Light is better,” *Optics and Photonics News*, May 1998, pp. 28–32.

Chynoweth, A.G. “Lightwave Communications: The fiber lightguide,” *Physics Today*, 29 (5), 28, 1976.

Farmer, K.R., and T.G. Digges. “A miniature fiber sensor,” *Photonics Spectra*, August 1996, pp. 128–129.

"Fiber Optic Technology Put to Work—Big Time," *Photonics Spectra*, August 1994, p. 114.

Gambling, W.A. "Glass, light, and the information revolution, Ninth W.E.S. Turner Memorial Lecture," *Glass Technology*, Vol. 27 (6), 179, 1986.

Ghatak, A., I.C. Goyal, and R. Varshney. *Fiber optica: A software for characterizing fiber and integrated optic waveguides*. New Delhi: Viva Books, 1999.

Ghatak, A., and K. Thyagarajan. *Introduction to fiber optics*. Cambridge: Cambridge University Press, 1998.

Grifford, R.S., and D.J. Bartnik. "Using optical sensors to measure arterial blood gases," *Optics and Photonics News*, March 1998, pp. 27–32.

Hotate, K. "Fiber Optic Gyros," *Photonics Spectra*, April 1997, p. 108.

Ishigure, T., E. Nihei, and Y. Koike. "Optimum refractive index profile of the graded index polymer optical fiber, toward gigabit data links," *Applied Optics*, Vol. 35, 1996, pp. 2048–2053.

Kao, C.K., and G.A. Hockham. "Dielectric-fibre surface waveguides for optical frequencies, *Proc. IEEE*, Vol. 113 (7), 1151, 1966.

Kapron, F.P., D.B. Keck, and R.D. Maurer. "Radiation losses in glass optical waveguides," *Applied Physics Letters*, Vol. 17, 423, 1970.

Katzir, A. "Optical Fibers in Medicine," *Scientific American*, May 1989, pp. 86–91.

Keiser, G. *Optical Fiber Communications*. New York: McGraw Hill, 1991.

Koeppen, C., R.F. Shi, W.D. Chen, and A.F. Garito. "Properties of plastic optical fibers," *Journal of the Optical Society of America*, B Vol. 15, 1998, 727–739.

Koike, Y., T. Ishigure, and E. Nihei. "High bandwidth graded index polymer optical fiber," *IEEE Journal of Lightwave Technology*, Vol. 13, 1995, pp. 1475–1489.

Maclean, D.J.H. *Optical Line Systems*. Chichester: John Wiley, 1996.

Marcou, J., M. Robiette, and J. Bulabois. *Plastic Optical Fibers*, Chichester: John Wiley and Sons, 1997.

Marcuse, D. "Loss analysis of single mode fiber splices," *Bell Systems Tech. Journal*, Vol. 56, 703, 1977.

Miya, T., Y. Terunama, T. Hosaka, and T. Miyashita. "An ultimate low loss single mode fiber at 1.55 mm," *Electron. Letts*., Vol. 15, 106, 1979.

"Schott is lighting the way home," *Fiberoptic Product News*, February 1997, p. 13.

Spillman, W.B., and R.L. Gravel. "Moving fiber optic hydrophone," *Optics Letters*, Vol. 5, 1980, 30–33.

